NASA/TM—2003-212515

Probabilistic Evaluation of Advanced Ceramic Matrix Composite Structures

Galib H. Abumeri
QSS Group, Inc., Cleveland, Ohio

Christos C. Chamis
Glenn Research Center, Cleveland, Ohio

July 2003

The NASA STI Program Office . . . in Profile

Since its founding, NASA has been dedicated to the advancement of aeronautics and space science. The NASA Scientific and Technical Information (STI) Program Office plays a key part in helping NASA maintain this important role.

The NASA STI Program Office is operated by Langley Research Center, the Lead Center for NASA's scientific and technical information. The NASA STI Program Office provides access to the NASA STI Database, the largest collection of aeronautical and space science STI in the world. The Program Office is also NASA's institutional mechanism for disseminating the results of its research and development activities. These results are published by NASA in the NASA STI Report Series, which includes the following report types:

- TECHNICAL PUBLICATION. Reports of completed research or a major significant phase of research that present the results of NASA programs and include extensive data or theoretical analysis. Includes compilations of significant scientific and technical data and information deemed to be of continuing reference value. NASA's counterpart of peer-reviewed formal professional papers but has less stringent limitations on manuscript length and extent of graphic presentations.

- TECHNICAL MEMORANDUM. Scientific and technical findings that are preliminary or of specialized interest, e.g., quick release reports, working papers, and bibliographies that contain minimal annotation. Does not contain extensive analysis.

- CONTRACTOR REPORT. Scientific and technical findings by NASA-sponsored contractors and grantees.

- CONFERENCE PUBLICATION. Collected papers from scientific and technical conferences, symposia, seminars, or other meetings sponsored or cosponsored by NASA.

- SPECIAL PUBLICATION. Scientific, technical, or historical information from NASA programs, projects, and missions, often concerned with subjects having substantial public interest.

- TECHNICAL TRANSLATION. English-language translations of foreign scientific and technical material pertinent to NASA's mission.

Specialized services that complement the STI Program Office's diverse offerings include creating custom thesauri, building customized databases, organizing and publishing research results . . . even providing videos.

For more information about the NASA STI Program Office, see the following:

- Access the NASA STI Program Home Page at ***http://www.sti.nasa.gov***

- E-mail your question via the Internet to help@sti.nasa.gov

- Fax your question to the NASA Access Help Desk at 301–621–0134

- Telephone the NASA Access Help Desk at 301–621–0390

- Write to:
  NASA Access Help Desk
  NASA Center for AeroSpace Information
  7121 Standard Drive
  Hanover, MD 21076

NASA/TM—2003-212515

Probabilistic Evaluation of Advanced Ceramic Matrix Composite Structures

Galib H. Abumeri
QSS Group, Inc., Cleveland, Ohio

Christos C. Chamis
Glenn Research Center, Cleveland, Ohio

National Aeronautics and
Space Administration

Glenn Research Center

July 2003

The Propulsion and Power Program at
NASA Glenn Research Center sponsored this work.

Available from

NASA Center for Aerospace Information
7121 Standard Drive
Hanover, MD 21076

National Technical Information Service
5285 Port Royal Road
Springfield, VA 22100

Available electronically at http://gltrs.grc.nasa.gov

TABLE OF CONTENTS

TABLES

FIGURES

SECTION 1. ABSTRACT

The objective of this report is to summarize the deterministic and probabilistic structural evaluation results of two structures made with advanced ceramic composites (CMC): internally pressurized tube and uniformly loaded flange. The deterministic structural evaluation includes stress, displacement and buckling analyses. It is carried out using the finite element code MHOST[1], developed for the 3-D inelastic analysis of structures that are made with advanced materials. The probabilistic evaluation is performed using the integrated probabilistic assessment of composite structures computer code IPACS[2]. The affects of uncertainties in primitive variables related to the material, fabrication process, and loadings on the material property and structural response behavior are quantified. The primitive variables considered are: thermo-mechanical properties of fiber and matrix, fiber and void volume ratios, use temperature, and pressure. The probabilistic structural analysis and probabilistic strength results are used by IPACS to perform reliability and risk evaluation of the two structures. The results will show that the sensitivity information obtained for the two composite structures from the computational simulation can be used to alter the design process to meet desired service requirements. In addition to detailed probabilistic analysis of the two structures, the following were performed specifically on the CMC tube: (1) predicted the failure load and the buckling load, (2) performed coupled non-deterministic multi-disciplinary structural analysis, and (3) demonstrated that probabilistic sensitivities can be used to select a reduced set of design variables for optimization.

SECTION 2. INTRODUCTION

Advanced composite materials, such as CMC, are ideal for use in designing aerospace structural components because of their unique and essential characteristics such as high strength and stiffness, high use temperature, and low density. Designing with composites poses multifaceted challenges including multiscales of composites, durability, life, and effect of service environments. The difficulties in design are further compounded by inherent uncertainties in the thermo-mechanical material properties, structural geometry (shape), fabrication process variables, loading, and service environments. To account for various uncertainties and to satisfy diverse design requirements, safety factors are traditionally used. The use of safety factors reduces the design load of composite structures resulting in substantial weight and cost increases. Clearly, the need exists for an alternate method that quantifies the various uncertainties that naturally occurs in a composite structure. Hence, the effect of uncertainties in primitive variables can be quantified by using a computational simulation that combines probabilistic composite mechanics and probabilistic composite structural analyses.

The objective of the present investigation is to present methods/codes for simulating computationally the behavior and response of composite materials/structures by probabilistically assessing the effect of uncertainties on the structure. Two composite structures are considered in this investigation. The first is an internally pressurized tube and the second is a uniformly loaded flange. Each structure is evaluated deterministically first followed by detailed non-deterministic assessment. The deterministic evaluation includes stress, displacement and buckling analyses. Note that buckling analysis is performed only on the tube structure. The probabilistic evaluation of the CMC tube covered ply strength, ply stress, ply stress failure criterion, and buckling load. The probabilistic evaluation of the CMC flange covered ply stress, ply stress failure criterion, and nodal displacement. The primitive variables considered in this evaluation for the two structures

are: modulus, thermal expansion coefficient and strength of fiber and matrix, fabrication process variables (fiber and void volume ratios), use temperature, and pressure. The probabilistic sensitivity factors are computed to provide quantifiable information on the relative sensitivity of material and structural primitive variables on the respective performance of the structure. Next, results from the deterministic evaluation of the CMC tube are discussed.

SECTION 3. DETERMINISTIC STRUCTURAL EVALUATION OF CMC TUBE

A cross section of an internally pressurized CMC tube is shown in Figure 1. A ply layup of $[2(0,90),0]_s$ is used in configuring the CMC structure. The wall thickness of the tube is one tenth of one inch and the height of its cross-section is one inch. A section three inches long, supported on one end, is modeled using 96 four-noded shell elements with 128 nodes (six degrees of freedom per node). The fiber considered in this evaluation is Nextel 720 fiber and the matrix is Aluminosilicate. The fiber is supplied as a 1500 denier, 400 filament count tow woven into an 8HS balanced fabric. The Nextel 720 fiber consists of 50% alumina and 50% mulite by weight. The fiber weight density is 0.123 lb/in^3. The matrix consists of alumina particulates held together by a foamy silica with an estimated density of 0.115 lb/in3. The predicted fiber and matrix properties are listed in Table 1. The properties include fiber and matrix moduli, strength, and thermal expansion coefficients. Also Table 1 lists the fabrication process variables, which are: 45% fiber volume ratio and 10% void volume ratio. The tube is designed for the application of internal pressure of 30 psi. In order to determine the pressure that causes ply damage, stress analysis is performed repeatedly with various pressure rates until ply damage is detected. Based on the deterministic stress analysis, the initial ply damage does occur at an internal pressure equal to or greater than 157.5 psi. The simulation results obtained for the 30 and 157.5 psi internal pressures are based on an initial use temperature of 70 ºF and a composite cure temperature of 300 ºF. Nonetheless, to assess the effect of elevated use and cure temperatures on the performance of the CMC structure, ply failure is also re-evaluated at a use temperature of 2000 ºF and a composite cure temperature of 2200 ºF. The latter evaluation is a reasonable simulation because the composite structure stills needs to be fired at high temperature.

The resultant displacements for the internally pressurized tube are plotted in Figure 2 for an internal pressure of 157.5 psi. Note that the magnitude of the displacement is relatively small in magnitude where it was about 0.00135” for 157.5 psi pressure. Ply stress evaluation is performed and results obtained with an internal pressure of 157.5 psi are shown in Figure 3-a for longitudinal ply stress, Figure 3-b for transverse ply stress, and Figure 3-c for shear ply stress. The results presented pertain to ply number 9, which is the second ply from the top and is oriented at 90º. As it can be seen from the stress plots, the maximum longitudinal stress is about –1.25 ksi while the longitudinal compressive strength is about 82 ksi. The shear stress is very low (less than 50 psi) and does not pose any problem because the ply strength in the shear direction is about 5.7 ksi. But an evaluation of the ply transverse stress shows that deterministically, the ply transverse stress exceeded the strength limit of 5.7 ksi because the maximum transverse stress reached 6.3 ksi. Stress analysis focused on ply 9 only because it is the ply where initial failure is presumed to take place.

In addition to stress and displacement analyses, buckling[3] analysis is necessary to evaluate the overall stability and identify any local failure under design load conditions. To preserve the stability of the structure under given loads, the structure must possess the required geometric stiffness. Failure due to deficiency in geometric stiffness is estimated through detailed buckling

analysis. Using the state of stress under given load conditions, the geometric stiffness of the structure is calculated. Equation 1 of the Appendix in Section 12 shows how finite element methods can be used to perform buckling analysis. The eigenvalues and eigenvectors of the geometric stiffness define the buckling load and shape. Results from the deterministic buckling analysis of the internally pressurized tube indicate that the tube becomes unstable at an internal pressure of 120 psi. A three dimensional view of the first buckling mode shape is presented in Figure 4. It is worth noting that when the tube buckles, it would open up forcing the top and bottom radial cross-sections to collapse.

SECTION 4. FUNDAMENTAL CONSIDERATIONS FOR PROBABILISTIC EVALUATION

The fundamental concepts implemented in the probabilistic composite assessment described herein are (1) the scatter in the composite structures for the probabilistic assessment should be traced from top to the lowest scale of influence; (2) the identified uncertain variables are called the primitive variables and should include those resulting from the composite fabrication, material properties, and loads; (3) the scatter in all the primitive variables (described as the composite material, loads, and fabrication process) can be represented by specified probabilistic distributions; (4) these variables can be used in conjunction with composite mechanics and finite-element structural analysis to predict composite material and/or structural behavior; and (5) the simulation can be repeated many times to obtain sufficient information to develop the distribution of the ply property, composite property, and/or structural response.

The considered primitive variables for the two CMC structures at the various composite scales are (1) fiber and matrix thermo-mechanical properties at the fiber-matrix constituent scale; (2) fiber and void volume ratios; and (3) pressure load at the structural scale. The methodology developed for the assessment of composite structures has been embedded in the computer code IPACS. Figure 5 shows the physics forming the basis for the IPCAS code.

SECTION 5. DESCRIPTION OF PROBABILISTIC STRUCTURAL ANALYSIS COMPUTER CODE IPACS

The probabilistic structural analysis presented in this report is performed by using the integrated probabilistic assessment of composite structures computer code IPACS. With the direct coupling of composite mechanics, structural analysis, and probabilistic methods, IPACS is capable of simulating uncertainties in all inherent scales of the composite, from constituent materials to the composite structure and its loading conditions.

The evaluation process starts with the identification of the primitive variables at the micro and macro composites scales including fabrication. These variables are selectively perturbed in order to generate a database for the determination of the relationships between the desired materials behavior and/or structural response and the primitive variables. The composite micro-mechanics is used to carry over the scatter in the primitive variables to the ply and laminate scales (steps A and B in Figure 5). Laminate theory is then used to determine the scatter in the material behavior at the laminate scale (step C). This step leads to the perturbed resultant force/moment-displacement/curvature relationships used in the structural analysis. Next, the finite element analysis is performed to determine the perturbed structural responses

corresponding to the selectively perturbed primitive variables (step D). This completes the description of the hierarchical composite material/structure synthesis shown on the left side of Figure 5. The multi scale progressive decomposition of the structural response to the laminate, ply, and fiber-matrix constituent scales is shown on the right side of Figure 5 (steps E to G). After the decomposition, the perturbed fiber, matrix, and ply stresses can be determined. An important feature of IPACS, depicted at the bottom of Figure 5, is the nonlinear multifactor interaction model for computing the fiber-matrix constituent material properties, including the effects of the prevailing service environments.

Next, the fast probability integrator (FPI[4]) code is used to determine the functional relationship between the response and the primitive variables. The cumulative distribution function of the response is then calculated with the numerically determined functional relationship and the known probability density functions of the primitive variables. The sensitivity factors of the primitive variables to each response's cumulative probability are also determined. This information is crucial for the reliability assessment.

The use of the computational simulation method that is presented in this report is a valuable tool for assessing reliability of composite structures. It can be used as an approach to satisfy design requirements. The effectiveness of the computational simulation is demonstrated using two structures: internally pressurized CMC tube and uniformly loaded CMC flange.

SECTION 6. PROBABILISTIC STRUCTURAL EVALUATION OF CMC TUBE

Uncertainties associated with thermo-mechanical material properties, fabrication variables, use temperature, and internal pressure, are assessed in this probabilistic simulation. Mean values, coefficient of variations, standard deviations, and assumed probability distributions for a total of 13 primitive variables are listed in Table 2. The material primitive variables are: fiber and matrix moduli, fiber and matrix thermal expansion coefficients, and fiber and matrix strength. The fabrication primitive variables are limited to the fiber volume ratio and the void volume ratio. The uncertainty in the load is simulated through the perturbation of the use temperature and the internal pressure. For the simulation results presented in this report, the composite cure temperature is not perturbed. The cure temperature is held fixed at 300 ºF for most cases. To assess the effect of elevated use and cure temperatures, the ply failure evaluation is repeated with a mean use temperature of 2000 ºF and a cure temperature of 2200 ºF. Note that the results presented in Section 6.1 through Section 6.8, are obtained based on a mean use temperature of 70 ºF and a cure temperature of 300 ºF. But the ply failure results presented in Section 6.9, are re-evaluated with a mean use temperature of 2000 ºF and a cure temperature of 2200 ºF. Through this process, it will be demonstrated that there exist a methodology for the probabilistic assessment of the structural performance of advanced composite structures. The innovative computational simulation presented in this report is capable of assessing reliably and efficiently the performance of any composite structure under various use conditions.

6.1 Evaluation of Ply Longitudinal strength

The deterministic evaluation of the ply longitudinal tensile and compressive strength is obtained with the use of equations 2 and 3 of the Appendix in Section 12. IPACS is used to evaluate probabilistically the longitudinal tensile and compressive strength. Results from the probabilistic analysis are plotted for ply 9, the ply that is oriented at 90º (second ply from the top). Strength for ply 9 is selected for evaluation because it is the ply where failure is initiated, as

it will be demonstrated later in this report. The cumulative distribution function for the ply longitudinal tensile and compressive strength is plotted in Figure 6. The mean longitudinal tensile strength is 138.6 ksi while the mean compressive longitudinal strength is 82.1 ksi. The tensile strength corresponding to 0.001 and 0.999 probabilities is 75 and 202 ksi, respectively. The compressive strength corresponding to 0.001 and 0.999 probabilities is 58 and 107 ksi. The probabilistic strength can be used to assess the reliability with respect to the required strength. For example, if the design reliability is set at 0.999 with required compressive strength of 100 ksi (less than 107 ksi), the failure probability will be less than 0.001. However, if the required strength is set at 120 ksi (greater than 107 ksi), the failure probability will be greater than 0.001.

The probabilistic sensitivities for the ply longitudinal tensile strength are plotted in Figure 7. Sensitivity results show that the fiber tensile strength and fiber volume ratio are the dominant uncertainties in that order. The fiber volume ratio sensitivity is decreased from 0.65 at a probability of 0.001 to 0.365 at probability of 0.999. The effect of the fiber volume ratio on the ply strength lessens as the cumulative probability increases. Other important information from the sensitivity analysis is that the void volume ratio has a negligible effect and it cannot be used to control the scatter in the tensile strength.

The probabilistic sensitivity analysis results for the compressive strength are plotted in Figure 8. The primitive variables that affect the ply longitudinal compressive strength are in the order: matrix shear strength, void volume ratio, fiber volume ratio, and matrix tensile strength. The fiber compressive strength has a negligible effect on the scatter of the ply compressive longitudinal strength. Note that the remaining primitive variables have no effect at all on the ply strength. If the failure of the structure is controlled by the ply longitudinal compressive strength, it would a waste of resources to focus on improving the fiber and matrix moduli, fiber and matrix thermal expansion coefficients, fiber tensile strength, use temperature and pressure loading. Sensitivity analysis is a powerful approach to identify the primitive variables that control the scatter in the response at hand (longitudinal ply strength).

It is important to note that throughout the investigative study that is presented in this report, the use temperature sensitivity effect is negligible (near zero). The use temperature at the selected level of 70 ºF does not influence the structural response whether the response is strength, stress, displacement, and buckling load. If the use temperature is elevated, then the response would likely be affected by uncertainty in the temperature.

6.2 Evaluation of Ply Transverse Strength

Results from the probabilistic evaluation of ply 9 transverse strength are summarized in Figures 9 and 10. The probabilistic transverse tensile strength is equal to the compressive one because the matrix tensile and compressive strength have the same mean values, standard deviations, and probabilistic distributions. Micromechanics equations used in the evaluation of the ply transverse strength are available in the Appendix (equations 4 and 5). With a mean strength of 5.7 ksi, the 0.001 and 0.999 probabilities transverse strength are 4.75 and 6.9 ksi, respectively. The probabilistic sensitivities shown in Figure 10 indicate that the tensile matrix strength has the largest effect on the transverse strength followed by the void volume ratio and the fiber volume ratio. To reduce the variation in the transverse strength, the scatter in the matrix strength and fabrication variables should be controlled. The effect of the matrix strength is greater at high probability than that of low probability. The matrix strength sensitivity increased from 0.77 (at 0.001 probability) to 0.90 (at 0.999 probability). The void volume ratio sensitivity is reduced from 0.57 (at 0.001 probability) to 0.40 (at 0.999 probability). When the sensitivity of

a primitive variable varies from one probability level to the other, it indicates that the relationship between the structural response and the primitive variable is nonlinear.

6.3 Evaluation of Ply Shear Strength

The micromechanics equation for the in-plane shear strength is presented in the Appendix (equation 6). Results from the probabilistic evaluation of ply 9 shear strength are presented in Figures 11 and 12. The cumulative probability is plotted against the probabilistic strength in Figure 11. The mean shear strength is the same as the transverse strength of 5.7 ksi. The shear strength is 4.7 ksi at 0.001 probability and is 6.90 ksi at 0.999 probability. The probabilistic sensitivities shown in Figure 12 indicate, as in the case of the probabilistic transverse strength, that variation in the ply shear strength is affected by the scatter in the matrix shear strength, void volume ratio, and fiber volume ratio. The 0.999 probability sensitivity factors are 0.9 for the matrix shear strength; 0.38 for the void volume ratio; and 0.2 for the fiber volume ratio.

6.4 Evaluation of Ply Longitudinal Stress (30 psi pressure)

A plot of the probabilistic longitudinal stress as a function of the cumulative probability is depicted in Figure 13. The probabilistic stress is plotted at three locations ("a", "b", and "c") on the tube's circumference. This particular evaluation is based on using a mean internal pressure of 30 psi (same as the design pressure). It is clear from the plot that the longitudinal stress does not vary much on the tube's circumference. The 0.001 probability stress is estimated at –2.1 ksi and the 0.999 probability stress is estimated at 2.25 ksi. Note that the 50% probability stress is about -0.3 ksi. As it was shown in section 6.1, the mean longitudinal strength was found to be about 138.6 ksi in the tensile direction and 82 ksi in compression. Since the ply stress is very low in comparison to the strength, longitudinal ply failure is not possible in this case. Sensitivity plots for the longitudinal stress are presented in Figure 14. It is interesting to note that the dominant uncertainties are those of the fiber thermal expansion coefficient in the longitudinal direction followed by the matrix thermal expansion coefficient with sensitivity factor of 0.97 and 0.16 at 0.999 probability, respectively.

6.5 Evaluation of Ply Transverse Stress (30 psi pressure)

The probabilistic transverse stress results obtained with a mean internal pressure of 30 psi are shown in Figure 15. The stress is computed at three locations on the tube's circumference. Note that the transverse stress is higher at locations "a" and "b" than the one predicted at location "c". The magnitude of the stress at location "a" is very close to the one obtained at location "b" because of symmetry. The probabilistic transverse stress at location "a" and "b" vary from –1 ksi at low probability to 3 ksi at high probability. The stress at location "c" ranges from –1 ksi at low probability to 2.1 ksi at high probability. The probabilistic sensitivities presented in Figure 16 show that the fiber thermal expansion coefficient, internal pressure, and matrix thermal expansion are the dominant uncertainties in that order. The fiber and matrix moduli have a negligible effect on the ply transverse stress.

6.6 Evaluation of Ply Shear Stress (30 psi pressure)

The probabilistic ply shear stress results obtained with a mean internal pressure of 30 psi are presented in Figure 17. The ply shear stress is computed at three distinct locations on the tube's circumference. It is worth noting that the maximum shear stress at high probability does not exceed 120 psi. Therefore, with the level of shear stress at the 30 psi mean design load, it is unlikely for the ply to fail in shear at higher loads because the stress to strength ratio is very small.

The probabilistic sensitivities results are presented in Figure 18. The fiber thermal expansion coefficient has the most dominant uncertainty with sensitivity of 0.97 at 0.999 probability followed by the matrix thermal expansion. The second dominant primitive variable is the matrix thermal expansion coefficient (moderate sensitivity) followed by the fiber and matrix moduli (low sensitivity).

6.7 Evaluation of Combined Stress Failure (30 psi Pressure)

The combined stress failure criterion[5] can be evaluated deterministically through the use of equation 7 of the Appendix in Section 12. When the combined stress failure criterion has a numerical value less than one, it indicates that the ply will not fail, equals to one indicates that failure is imminent, and greater than one indicates that the ply already failed. . Note that throughout the probabilistic evaluation of the CMC tube, the list of primitive variables and assumed standard deviations and probabilistic distribution remain unchanged, as defined in Table 2.

The cumulative probability for the combined stress failure criterion is plotted in Figure 19. As in the case of the transverse stress, the failure criterion is computed at three locations on the tube's circumference. The ply with the largest failure criterion is plotted at location "a", "b", and "c". Note that with a mean internal pressure of 30 psi and due to symmetry, the value of the failure function at "a" and "b" are identical. A maximum value of 0.30 is obtained for the combined stress failure criterion at a probability of 0.999. The same function evaluated at location c on the tube's circumference resulted in a maximum function value of 0.10 at high probability. It is clear from the probabilistic analysis that no ply failure will occur because the failure function is less than 1.0. As a result of this analysis, the tube will be re-assessed at higher internal pressure load.

The probabilistic sensitivity results are presented in Figure 20. With an internal pressure of 30 psi, the primitive variables that affect the combined stress failure criterion are in the order of importance: fiber thermal expansion coefficient (high); matrix thermal expansion coefficient, matrix tensile strength, and internal pressure (moderate); and void and fiber volume ratios, and fiber and matrix moduli (low).

6.8 Evaluation of Ply Transverse Stress (157.5 psi Pressure)

As discussed in previous sections, the longitudinal and shear ply stresses are much lower than the allowable strength limits at design conditions. But with a mean transverse strength of 5.7 ksi, the ply transverse stress could rapidly approach the strength limit as the pressure increases. The transverse stress ranged from –1 ksi (at low probability) to 3 ksi (at high probability) when design load of 30 psi is applied. Additional analysis showed that the ply failure would occur at an internal pressure of 157.5 psi, that is 5.25 times the design pressure of 30 psi. The ply transverse stress is revaluated probabilistically by computing its cumulative distribution function and sensitivity of the primitive variables to the scatter range. A plot of the probabilistic transverse stress as a function of the cumulative probability is depicted in Figure 21. As done previously, the probabilistic stress is plotted at three locations ("a", "b", and "c") on the tube's circumference. Note that the transverse stress is higher at locations "a" and "b" than the one predicted at location "c". The magnitude of the probabilistic stress at location "a" is very close to the one obtained at location "b" because of symmetry. The mean stress at location "b" is 6.1 ksi and 4.2 ksi at location c. The probabilistic transverse stress at location "b" is 1.3 ksi at 0.001 probability and 9 ksi at 0.999 probability. Note that the 9^{th} ply at location "b" would fail at 0.50 probability because a transverse stress of 6.1 ksi exceeded the transverse strength of 5.7 ksi.

The probabilistic sensitivities presented in Figure 22 show that the internal pressure is the primitive variable that affects the transverse stress the most followed by the fiber thermal expansion coefficient. The matrix modulus and matrix thermal expansion coefficient have a moderate effect on the stress while the effect of the fabrication variables is negligible. To reduce the probability of failure, the scatter in the internal pressure must be controlled. Note that a mean internal pressure of 157.5 psi with a coefficient of variation of 15% is assumed for this investigation. The importance of the load (internal pressure) increased from a sensitivity of 0.3 at 0.001 probability with 30 psi pressure to 0.75 with 157.5 psi pressure.

6.9 Evaluation of Combined Stress Failure Criterion (157.5 psi Pressure)

The combined stress failure criterion cumulative probability obtained with a mean internal pressure of 157.5 psi, mean use temperature of 70 °F, and cure temperature of 300 °F is plotted in Figure 23-a. As in the case of the transverse stress, the failure criterion is computed at three different locations on the tube's circumference. The ply with the largest failure criterion is plotted at location "a", "b", and "c". Note that with a mean internal pressure of 157.5 psi, failure is imminent in the 9^{th} ply at location "b". It is interesting to observe that the value of the combined stress failure criterion at 0.001 probability is –0.8 at location "b", –0.76 at location "a", and –0.48 at location "c". To design for high reliability (0.999), the allowable combined stress failure function should not exceed the aforementioned numerical values.

The probabilistic sensitivities of the combined stress failure criterion to the scatter range at ply 9 of location "b" are presented in Figure 23-b. The primitive variable that affects the combined stress the most is the internal pressure followed by the fiber's thermal expansion coefficient and matrix transverse strength. The void volume ratio, matrix modulus, and matrix thermal expansion coefficient have moderate to low effect on the combined stress failure criterion. Failure can be minimized if the scatter in the internal pressure, fiber thermal expansion coefficient, and matrix transverse strength is controlled. The change in the sensitivity of the pressure load is consistent with the physical phenomena of failure. When a particular ply fails, it does so as a result of increase in transverse stress because of higher internal pressure load.

The combined stress failure criterion is also re-evaluated probabilistically using elevated use and cure temperatures. The re-evaluation is carried out based on a mean use temperature of 2000 ºF and a composite cure temperature of 2200 ºF. The combined stress failure criterion cumulative distribution function is plotted in Figure 24-a for the locations: "a", "b", and "c". It is appropriate to compare the results summarized in Figure 24-a to those presented in Figure 23-a. At 50% probability, ply 9 (90º) at location "a" has failed because its magnitude increased from 0.95 (at low use and cure temperatures) to 1.44 (at elevated use and cure temperatures). Note that failure is imminent when the combined stress failure criterion magnitude reaches 1.0. In addition, the 50% probability failure criterion at locations "b" and "c" have also increased from 0.99 at "b" to 1.51 and from 0.47 at "c" to 0.78" when elevated use and cure temperatures are introduced. It is worth noting that the use of elevated use and cure temperatures leads to an increase in the scatter range of the combined stress failure criterion as shown in Figure 24-a. Also, higher use and cure temperatures produce ply failure, deterministically and probabilistically, earlier than that in the case of lower use and cure temperatures.

The combined stress failure criterion probabilistic sensitivities obtained with the elevated use and cure temperatures are summarized in Figure 24-b for ply 9 (90º) at location "b". The results presented can be compared to those of Figure 23-b., where lower use and cure temperatures were used. Note raising the mean use temperature from 70 ºF to 2000 ºF results in the increase of the probabilistic sensitivity by 30%. Also, the sensitivity of the fiber modulus increased 11% while

the sensitivity of the void volume ratio decreased 50%. The fiber thermal expansion coefficient sensitivity is lowered from 55% to 43% while the sensitivity of the matrix tensile strength and internal pressure remained unchanged at 50% and 65%, respectively. It is evident that the scatter in the mean use temperature of 2000 ºF plays an important role in preventing ply failure. The ability to quickly evaluate the performance of a structure with various use and cure temperatures demonstrate the effectiveness of the computational methodology that is described in this report.

The probabilistic sensitivity results obtained for the combined stress failure criterion at location "b" are carried further by examining the values of the primitive variables at three distinct probability levels: 0.001, 0.50, and 0.999. The primitive variables corresponding to any probability is known as the Most Probable Design (MPP) at that probability. Figure 25 shows the normalized value of the MPP for all thirteen primitive variables. Again, the results are consistent with the physics of the problem. At 0.001 probability, the failure function is about –0.8 indicating "no failure". The internal pressure that corresponds to the 0.001 probability is about 102 psi (65% of the mean pressure of 157.5 psi). Note that the pressure that corresponds to 0.999 probability is about 220 psi (140% of the mean pressure of 157.5 psi). Failure is imminent at a 0.999 probability because the combined stress failure criterion exceeded the limit value of 1.0 (it was around 2.6). Decrease in the load yields a safer design (no failure) and increase in the load causes failure.

In addition to examining the MPP at three probabilities, the tube is analyzed deterministically using conditions at the 0.001, 0.50, and 0.999 probabilities. Ply transverse stress is evaluated for the three probabilities and finite element plots are presented in Figures 26-a through 26-c. Note that failure is imminent at 0.999 probability because the maximum transverse stress of 8.5 ksi exceeds the strength limit of 6.9 ksi at that probability by 25%. The deterministic evaluation based on probabilistic design is a further confirmation that the probabilistic sensitivities can be used to control the scatter in the primitive variables that contribute most to failure.

6.10 Evaluation of Buckling Load

The probabilistic assessment of the combined failure stress that was presented earlier, checks the failure in the material. But failure due to deficiency in geometric stiffness is assessed through detailed probabilistic buckling analysis. Probabilistic buckling analysis is performed using the primitive variables listed in Table I. The cumulative distribution function for the buckling load of the CMC tube is shown in Figure 27. Reliability based design requires a lower value of probability of occurrence of the buckling load. For a design cumulative probability of 0.001 (reliability of 0.999), the design load should be less than 36 psi. The buckling load at 0.001 and 0.999 cumulative probabilities is most sensitive to the internal pressure followed by the fiber volume ratio. The matrix modulus, fiber modulus, and void volume ratio have moderate to low effect on the buckling load. As shown in Figure 28, the probabilistic sensitivity analysis asserts that the scatter in the fiber and matrix thermal expansion coefficients, strength, and use temperature (at the selected level) have no effect on the buckling load. As demonstrated here, sensitivity analysis is of extreme importance because it highlights the primitive variables that are most critical to the buckling load.

SECTION 7. DETERMINISTIC STRUCTURAL EVALUATION OF CMC FLANGE

As mentioned in Section 1 of this report, the structural evaluation is performed for two structures: internally pressurized CMC tube and uniformly loaded CMC flange. Deterministic

and probabilistic simulation results were presented in previous sections for the CMC tube. The second structure that is considered for structural evaluation is a uniformly loaded CMC flange. The flange has an attachment height of one inch and a length on 2.5 inches. As it is shown in Figure 29, a total of three ply groups are used in defining the material configuration of the flange. They are distinctly identified by the letters: (a) for the layup [90,–45,45,0]; (b) for the layup [2(0,–45,45,90),(90,45,–45,0)]; and (c) for the layup [2(0,–45,45,90),2(90,45,–45,0)]. Note that as it is indicated in Figure 29, most of the flange is made up of layup group (c) with the other two ply groups used in defining the transition region from the vertical wall to the horizontal surface. The fiber and matrix used are the same as the ones used for the CMC tube: Nextel 720 fiber and Aluminosilicate matrix. The thermo-mechanical properties of the fiber and matrix are summarized in Table 1. Also Table 1 lists the fabrication process variables: 45% fiber volume ratio, 10% void volume ratio, and cure temperature for 300 ºF.

The flange is subjected to a uniform pressure of 15 psi. A finite element model of the flange is shown in Figure 29. The number of shell elements that is used in modeling the flange is 117 with 156 nodes. Displacement analysis is performed using the finite element code MHOST. The resultant displacements obtained from the deterministic evaluation are presented in Figure 30. A maximum displacement of 0.0016 inch is detected at the free end of the flange. Although the displacements are finite, a detailed ply stress analysis is required to ensure no failure in the material under applied design loads. Longitudinal, transverse and shear ply stress results are shown for the top ply in Figure 31-a through Figure 31-c. The stress analysis results show that the longitudinal stress varied from –22 ksi to 40 ksi with a compressive strength of 86 ksi and a tensile strength of 138 ksi. With shear and transverse strength of 5.7 ksi, the transverse stress for the same ply varied from –3.8 ksi to 17.7 ksi while the shear stress varied from –7 ksi to 13 ksi. It is clear that for the top ply, failure is imminent in both transverse and shear directions. The results discussed in this section underscore the need to perform probabilistic evaluation to come up with a guideline on what primitive variables can be controlled if ply failure is to be prevented when design loads are applied.

SECTION 8. PROBABILISTIC STRUCTURAL EVALUATION OF CMC FLANGE

Uncertainties effects of thermo-mechanical material properties, fabrication variables, use temperature, and pressure on the structural response of the CMC flange are assessed using the probabilistic simulation code IPACS. Mean values, coefficient of variations, standard deviations, and assumed probability distributions for a total of 13 primitive variables are listed in Table 2 (same as the ones used for the tube problem). The uncertainty in the load is simulated through the perturbation of the use temperature and the uniform pressure. It is important to note that the only difference between the primitive variables that are used in assessing the tube structure and the ones used in the assessment of the CMC flange is the magnitude of the mean pressure, which is set to 15 psi for the flange structure. With a 15% coefficient of variation, the standard deviation for the pressure is found to be 2.25 psi.

8.1 Evaluation of Ply Longitudinal Stress

The probabilistic evaluation of the CMC flange ply longitudinal stress is depicted in the plots in Figure 32. The cumulative distribution function at three distinct locations on the flange (locations “a”, “b”, and “c”) are plotted against the probabilistic ply longitudinal stress. Locations “a” and “b” are in the area where the flange transitions from vertical wall to horizontal surface.

Location “c” is in the area of the vertical wall right where the flange is attached. The probabilistic results presented are for ply 2 (–45º ply) at location “a”, ply 9 (90º ply) at location “b”, and ply 1 (0º ply) at location “c”. There are two reasons for selecting different plies at various locations: (1) to show that the assessment can be done at any ply or all plies in the structure, and (2) because the selected plies had the largest combined stress effect thru those specific locations or nodes. As shown in Figure 32, the ply longitudinal stress at location “c” had the scatter of 7.8 ksi (at 0.001 probability) to 19.7 ksi (at 0.999 probability). The scatter in the stress at location “c” is the largest of all three locations (“a”, “b”, and “c”). It is worth noting that the selected plies will not fail in the longitudinal direction because the stress level is much less than the ply strength limit in the longitudinal direction of 138 ksi.

The probabilistic sensitivities results are presented in Figure 33. The analysis shows that the fiber thermal expansion coefficient in the longitudinal direction has the largest effect on the longitudinal stress (sensitivity of 0.97). The thermal effect is resulting from the 300 ºF cure temperature and use temperature of 70 ºF. The matrix thermal expansion coefficient, matrix modulus, pressure and fiber modulus had a negligible effect on the structural response (longitudinal stress). If failure was to occur due to high stress in the longitudinal direction, than the uncertainty in the fiber thermal expansion coefficient could be controlled due to minimize the scatter in the longitudinal stress.

8.2 Evaluation of Ply Transverse Stress

The probabilistic analysis results for the CMC flange ply transverse stress are presented in Figure 34. The cumulative distribution function at locations “a”, “b”, and “c” are plotted against the probabilistic ply transverse stress. As shown in Figure 34, the ply transverse stress at location “a” (–45º ply) had a scatter of 11.5 ksi (at 0.001 probability) to 17 ksi (at 0.999 probability), that is about 5.5 ksi. The scatter in the transverse stress at location “b” is about 2 ksi, while the scatter at location “c” is about 3.9 ksi. The stress magnitude at location “a” indicates that the ply failure is imminent because the lowest stress of 11.5 ksi exceeded the 0.001 probabilistic transverse strength of 4.7 ksi. Here the ply failure probability is greater than 0.999. Also, failure is likely to occur for the ply at location “c” (0º ply) because the stress level at 0.001 probability is about 6.4 ksi which exceeds the strength limit of 4.7 ksi.

The probabilistic sensitivities results are presented in Figure 35. The analysis shows that the fiber volume ratio has the largest effect on the transverse stress (sensitivity of 0.78) followed by the matrix modulus (sensitivity 0.58) and the matrix thermal expansion coefficient (sensitivity 0.48). The void volume ratio, fiber thermal expansion coefficient, and pressure have a negligible effect on the ply transverse stress. Mainly, controlling the uncertainty in the fiber volume ratio, matrix modulus and matrix thermal expansion coefficient will surely minimize the scatter in the transverse stress, which might lead to the prevention of ply failure. The sensitivity analysis is definitely a unique and powerful outcome of the probabilistic evaluation because it can guide the designer to ensure exact tailoring of a structural component to meet specific operational requirements.

8.3 Evaluation of Ply Shear Stress

We just examined the effect of uncertainty of fiber and matrix thermo-mechanical properties, fabrication parameters, and loading on the longitudinal and transverse stress for selected plies. Now it is turn to evaluate the probabilistic shear stress for the same plies. The probabilistic analysis results for the CMC flange ply shear stress are presented in Figure 36. The cumulative distribution function at locations “a”, “b”, and “c” are plotted against the probabilistic ply shear

stress. The ply shear stress at location "a" (–45º ply) had a scatter of –3.4 ksi (at 0.001 probability) to –1.8 ksi (at 0.999 probability), that is about 1.6 ksi. The scatter in the shear stress at location "b" is about 0.5 ksi, while the scatter at location "c" is about 0.02 ksi. The ply stress evaluation indicates that ply failure due to shear stress is unlikely because the stress level is smaller than the strength limit in the shear direction.

The probabilistic sensitivities results for ply 2 at location "a" are presented in Figure 37. The analysis shows that the fiber volume ratio has the largest effect on the shear stress (sensitivity of 0.96). The void volume ratio and pressure have lower effect on the ply transverse stress with sensitivity factor of 0.15 for both primitive variables. Controlling the uncertainty in the fiber volume ratio will minimize the scatter in the shear stress. If failure due to shear stress is probable, one can use the fiber volume ratio to control/prevent the considered failure phenomena.

8.4 Evaluation of Ply Combined Stress Failure Criterion

The probabilistic analysis results for the CMC flange ply combined stress failure criterion are presented in Figure 38. The cumulative distribution function at locations "a", "b", and "c" are plotted against the probabilistic ply combined stress failure criterion. As discussed in Section 8.2, it is clear that ply failure due to transverse stress is imminent for the ply at location "a" and likely at location "c", because the 0.001 probability failure function is 7.9 for the ply at location "a" and 0.22 for the ply at location "c". As seen earlier, the 0.001 probability transverse stress at locations "a" and "c" had exceed the allowable strength. At location "b", the failure function varied from 0.045 at 0.001 probability to 0.419 at 0.999 probability, which means that the probability of failure of ply 9 at location "b" is definitely much less than 0.001.

The probabilistic sensitivities results for the ply combined stress failure criterion at location "a" are presented in Figure 39. The analysis shows that the fiber volume ratio and the matrix tensile strength have the largest effect on the combine stress failure criterion (sensitivity of 0.65). The matrix modulus has moderate effect (0.33 sensitivity), while the void volume ratio and matrix thermal expansion coefficient have lesser effect (about 0.2 sensitivity). It is interesting to observe the fact that the surface pressure has a sensitivity of only 0.10. The applied pressure coupled with other parameters such as the thermal expansion coefficients contribute to ply failure. The ply failure is caused by the combined effect of the loading, cure temperature, and lack of matrix strength. Preventing ply failure can be achieved by using a matrix that possesses higher strength.

8.5 Evaluation of End Displacement

The probabilistic analysis results for the CMC flange free end displacement (in the direction of the applied pressure) are presented in Figure 40. The cumulative distribution function at the free end is plotted against the probabilistic displacement. The probability of having a displacement of –0.00038" is 0.001 and the probability of having a displacement of 0.00035" is 0.999. The pressure is 21.95 psi at 0.001 probability, 15 psi at 0.50 probability, and 8.05 psi at 0.999 probability. The probabilistic sensitivities results are shown in Figure 41. It is clear from the results that the only way to control the displacement at the free end of the flange is by controlling the scatter in the pressure. The sensitivity analysis results are consistent with the physics of the problem. Other important parameters would have affected the displacement if they were considered as primitive variables in the probabilistic evaluation. These parameters include the thickness of the flange and its width and length.

SECTION 9. MULTI-DISCIPLINARY PROBABILISTIC EVALUATION OF CMC TUBE

The purpose of this section is to demonstrate that a readily available computational simulation system can be used for the multi–disciplinary probabilistic evaluation of composite structures. Also, it will be shown that information from probabilistic analysis can be used to select design variables for optimization from a wide array of primitive variables. Probabilistic sensitivities are an effective way of identifying the primitive variables that are critical to the evaluation of a typical objective function such weight, cost, and reliability.

9.1 Description of EST/BEST

Recent research activities at NASA Glenn Research Center have focused on developing multi-scale, multi-level, multi-disciplinary analysis and optimization methods. Multi-scale refers to formal methods which describe complex material behavior; multi-level refers to integration of participating disciplines to describe a structural response at the scale of interest; multi-disciplinary refers to open-ended for various existing and yet to be developed disciplines. For example, these include but are not limited to: multi-factor models for material behavior, multi-scale composite mechanics, general purpose structural analysis, progressive structural fracture for evaluating durability and integrity, noise and acoustic fatigue, emission requirements, hot fluid mechanics, heat-transfer and probabilistic simulations. Many of these, as well as others, are encompassed in an integrated computer code identified as Engine Structures Technology Benefits Estimator (EST/BEST[6]). The discipline modules integrated in EST/BEST include: engine cycle (thermodynamics), engine weights, internal fluid mechanics, cost, mission and coupled structural\thermal, various composite property simulators and probabilistic methods to evaluate uncertainty effects (scatter ranges) in all the design parameters.

The EST/BEST (Engine Structures Technology Benefits Estimator) software, shown in Figure 42, is used to carryout the investigative study presented in this section. Component as well as system evaluations are performed within one single software. The modules included are integrated computer codes with multiple functional capabilities. The ones that are used for the results to be presented later in this section are (1) Cosmo for finite element generation; (2) Material Library - for composite mechanics simulation; (3) IPACS for composite structures probabilistic evaluation and (4) CSTEM[7] for coupled structural/thermal analysis and Optimization.

9.2 Coupled Deterministic Structural-Thermal Analysis of CMC Tube

The coupled structural-thermal analysis of the CMC duct is carried out using the CSTEM code in EST/BEST. The duct is subjected to an internal pressure of 50 psig and forced convection on its inner walls. The forced convection is based on the flow of hot air through the duct at a velocity of 0.2 MACH and a convection temperature of 3000 ºF. On the outside of the duct, free convection at 70 ºF is considered. Note that the maximum displacement obtained with the application of combined thermo-mechanical loading is about eight times higher than the one obtained with internal pressure only. Figure 43-a shows the deformation of the tube's cross-section under the effect of thermal load. The temperature distribution obtained for the composite duct from the thermal analysis is shown in Figure 43-b. The temperature varied from 2935 ºF on the inner walls of the duct to 2821 ºF on the outside. Next, the effect of uncertainties in thermo-mechanical properties and loads, and fabrication process parameters on the combined stress failure criterion will be assessed.

9.3 Coupled Probabilistic Structural-Thermal Analysis of CMC Tube

The effects of uncertainties in composite material properties, composite fabrication parameters, and combined thermo-mechanical loading are assessed. The combined stress failure criterion is evaluated probabilistically based on the following scatter in primitive variables: ±5% in fiber and matrix moduli, and convection temperature; ± 10% in fiber and matrix thermal conductivity, matrix thermal expansion coefficient, matrix strength, fiber volume ratio and heat transfer convection coefficient; and ±15% in fiber thermal expansion coefficient and fiber strength, void volume ratio, and internal pressure. The scatter ranges considered here are typical for the primitive variables selected in the study. The results from the probabilistic evaluation are presented in Figure 44. Note that for a probability higher than 0.92, failure is imminent. The probabilistic sensitivities of the combined stress failure criterion to the scatter range of the primitive variables are presented in figure 45. The objective of this particular evaluation is to identify the primitive variables critical to the failure of the CMC tube. The sensitivity analysis show that the void volume ratio, matrix tensile strength, convection temperature through the tube, internal pressure, and fiber volume ratio have the largest effect, in that order, on the failure stress of the tube. The thermal conductivities of fiber and matrix and thermal expansion coefficients have a negligible effect as indicated in Figure 45. Next, it will be demonstrated that the primitive variables list can be reduced to include only relevant design variables for use in optimization studies.

9.4 Use of Probabilistic Methods to Reduce Number of Design Variables in Optimization

Based on the probabilistic sensitivity analysis, the list of critical primitive variables can now be reduced to include matrix modulus, matrix thermal expansion coefficient, matrix conductivity, matrix strength, fiber volume ratios, and void volume ratio. If an optimization study is to be undertaken, the aforementioned primitive variables would be ideal for such a study. Although the primitive variables for loading show significant effects on the combined stress failure criterion, they are not recommended for inclusion in optimization. The loads are assumed to be constant with values of their respective means. Normally an aircraft structure is tailored to sustain a specific load range and the load itself is obtained from detailed aerodynamic analysis.

Figure 46 show the cumulative distribution function of the combined stress failure criterion with original and reduced set of primitive variables. The reduced set includes the matrix strength, void volume ratio, fiber volume ratio, matrix modulus, matrix thermal expansion coefficient, and matrix conductivity. Notice that the cumulative distribution function for the reduced set pivoted around the mean and shows less scatter than the whole set. Figure 47 shows the probabilistic sensitivities of the reduced set at two probability levels (0.001 and 0.999). The probabilistic sensitivities can be use as a guideline on what primitive variables to include or exclude for optimization. When the primitive variable has low sensitivity, less than 10%, it would be a waste of resources to consider it in an optimization study. One should focus on the primitive variables with uncertainties that affect greatly the structural response or objective function. Multidisciplinary non-deterministic optimization results are not included in this report. The reader may refer to reference 8 for details on the principle of non-deterministic optimization, as defined by the authors of this report.

SECTION 10. SUMMARY

A general and powerful method for comprehensive probabilistic assessment of composite structures was presented. The capabilities of the computational simulation method were demonstrated by assessing the reliability of an internally pressurized CMC tube and a uniformly loaded CMC flange. A specific list of major accomplishments is listed here:

1. The effect of uncertainties of thermo-mechanical properties, thermo-mechanical loadings, and fabrication process variables on the structural performance of the CMC tube and CMC flange are assessed with great level of details.
2. Predicted the probabilistic failure and buckling loads for the CMC tube.
3. Evaluated the probabilistic failure stress and probabilistic end displacement for the CMC flange.
4. Demonstrated that probabilistic sensitivities could be used to select a reduced set of design variables for optimization.

Comparable evaluation can readily be performed for other structural components/structures. The technology used here can be applied to perform reliability and risk assessment of these types of structures.

SECTION 11. REFERENCES

1. Nakazawa, S.; Nagtegaal, J.C.; and Wertheimer, T.B.: "3-D Inelastic Analysis Methods for Turbine Engine Hot Section Components, Special Finite Element Models: MHOST", MARC Research Corporation, Palo Alto, CA., version 4.2, 1987.
2. Chamis, C.C.; and Shiao, M.C.: "IPACS – Integrated Probabilistic Assessment of Composite Structures: Code Development and Applications". Third NASA Advanced Composite Technology Conference, Vol. 1, Pt. 2, NASA CP-3178-VOL-1-PT-2, 1993, pp. 987-999.
3. Shames, I.H.; and Dyma, C.L.: "Energy and finite Element Methods in Structural Mechanics", Hemisphere Publishing Corporation, pp. 632, 1985, New York.
4. Wu, Y.-T.: "Demonstration of a New Fast Probability Integration Method for Reliability Analysis", Advances of Aerospace Structural Analysis, ASME, pp. 63-73, 1985.
5. Murthy, P.L.N.; and Chamis, C.C.: "Integrated Composite Analyzer (ICAN): Users and Programmers Manual", NASA TP-2515, 1986.
6. Abumeri, G.H.; and Chamis, C.C.: "T/BEST a computer code for assessing the benefits of advanced aerospace technologies", published in the Advances in Engineering Software journal, pp. 231-238, 1997 Elsevier Science Limited, Printed in Great Britain.
7. Hartle, M.; and McKnight, R.L: CSTEM User Manual, NASA CR-2000-209308, January 2000.
8. Abumeri, G.H.; Kuguoglu, L.H.; and Chamis, C.C.: "Non-deterministic optimization—composite laminates, beams and blades", presented at the 41st AIAA/ASME/ASCE/AHS/ASC Structures, Structural and Materials Conference and Exhibit, Atlanta, GA, April 2000.

SECTION 12. APPENDIX: STRUCTURAL BUCKLING, PLY STRENGTH, AND PLY FAILURE EQUATIONS

Symbols

E	Young's Modulus
F	combined stress failure criterion
G	shear Modulus
K	stiffness matrix
k	volume fraction
S	strength
u	nodal displacement
α	coefficient of thermal expansion
β	coefficient of moisture expansion

Subscripts

C	compressive
F	flexural
G	geometric
f	fiber
l	ply or slice (subply)
m	matrix
T	tensile
v	voids
1	material axis, along the fiber
2,3	material axis, transverse to the fiber

Finite element solution for buckling[3] analysis:

$$([K_F] - \lambda[K_G])\{u\} = 0 \qquad [1]$$

All micromechanics equations are as defined in the Integrated Composite Analyzer code ICAN[5].

Ply longitudinal tensile strength:

$$S_{l11T} = S_{f11T}\left(k_f + k_m\left(E_m / E_{f11}\right)\right) \qquad [2]$$

Ply longitudinal compressive strength:

$$S_{FC11C} = S_{f11C}\left(k_f + k_m\left(E_m / E_{f11}\right)\right) \qquad [3]$$

Ply transverse tensile strength:

$$S_{l22T} = \left[1 - \left(\sqrt{k_f} - k_f\right)\left(1 - \frac{E_m}{E_{f22}}\right)\right] \text{ x } S_{mT}\left[1 - \sqrt{4k_v / \pi(1 - k_f)}\right] \qquad [4]$$

Ply transverse compressive strength:

$$S_{l22C} = \left[1 - \left(\sqrt{k_f} - k_f\right)\left(1 - \frac{E_m}{E_{f22}}\right)\right] \text{x } S_{mC}\left[1 - \sqrt{4k_v/\pi(1-k_f)}\right] \quad [5]$$

In-plane ply shear strength:

$$S_{l12S} = \left[1 - \left(\sqrt{k_f} - k_f\right)\left(1 - \frac{G_m}{G_{f12}}\right)\right] \text{x } S_{mS}\left[1 - \sqrt{4k_v/\pi(1-k_f)}\right] \quad [6]$$

Combined stress failure criterion:

$$F = 1 - \left(\frac{\sigma_{\ell 11\alpha}}{S_{\ell 11\alpha}}\right)^2 - \left(\frac{\sigma_{\ell 22\beta}}{S_{\ell 11\beta}}\right)^2 + K_{\ell 12}\frac{\sigma_{\ell 11\alpha}}{S_{\ell 11\alpha}}\frac{\sigma_{\ell 22}}{S_{\ell 22}} - \left(\frac{\sigma_{\ell 12S}}{S_{\ell 12S}}\right)^2 \quad [7]$$

Where $K_{\ell 12}$ is function of the material properties. The equation for $K_{\ell 12}$ is not listed here because it is too long. It can be found in reference 5.

Table 1. CMC tube fiber and matrix properties, fabrication parameters, and loading conditions

Fiber Modulus (msi)	**40**
Fiber's Poisson's Ratio (12)	**0.08**
Fiber's Poisson's Ratio (23	**0.08**
Fiber Thermal Expansion Coefficient (in/in/°F)	**2.4E-06**
Fiber Tensile Strength (ksi)	**300**
Fiber Compressive Strength (ksi)	**300**
Matrix Modulus (msi)	**4.4**
Matrix Poisson's Ratio	**0.21**
Matrix Thermal Expansion Coefficient (in/in/°F)	**3.25E-06**
Matrix Tensile Strength (ksi)	**13**
Matrix Compressive Strength (ksi)	**13**
Matrix Shear Strength (ksi)	**13**
Fiber Volume Ratio	**0.45**
Void Volume Ratio	**0.1**
Use Temperature (°F)	**70 and 2000**
Cure Temperature (°F)	**300 and 2200**
Internal Pressure (psi)	**15 and 157.5**

Table 2. Probabilistic modeling of internally pressurized CMC tube CMC

Primitive Variable	Mean Value	Coefficient of Variation (%)	Standard Deviation	Probabilistic Distribution
Fiber Modulus (msi)	40	5	2	Normal
Fiber Thermal Expansion Coefficient (in/in/°F)	2.4E-06	15	0.36E-06	LogNormal
Fiber Tensile Strength (ksi)	300	15	45	LogNormal
Fiber Compressive Strength (ksi)	300	15	45	LogNormal
Matrix Modulus (msi)	4.4	5	0.22	Normal
Matrix Thermal Expansion Coefficient (in/in/°F)	3.25E-06	10	0.325E-06	LogNormal
Matrix Tensile Strength (ksi)	13	10	1.3	LogNormal
Matrix Compressive Strength (ksi)	13	10	1.3	LogNormal
Matrix Shear Strength (ksi)	13	10	1.3	LogNormal
Fiber Volume Ratio	0.45	10	0.045	Normal
Void Volume Ratio	0.1	15	0.015	LogNormal
Use Temperature (°F)	70 2000	10 10	7 200	Normal Normal
Internal Pressure (psi)	30 157.5	15 15	4.50 23.625	Normal Normal

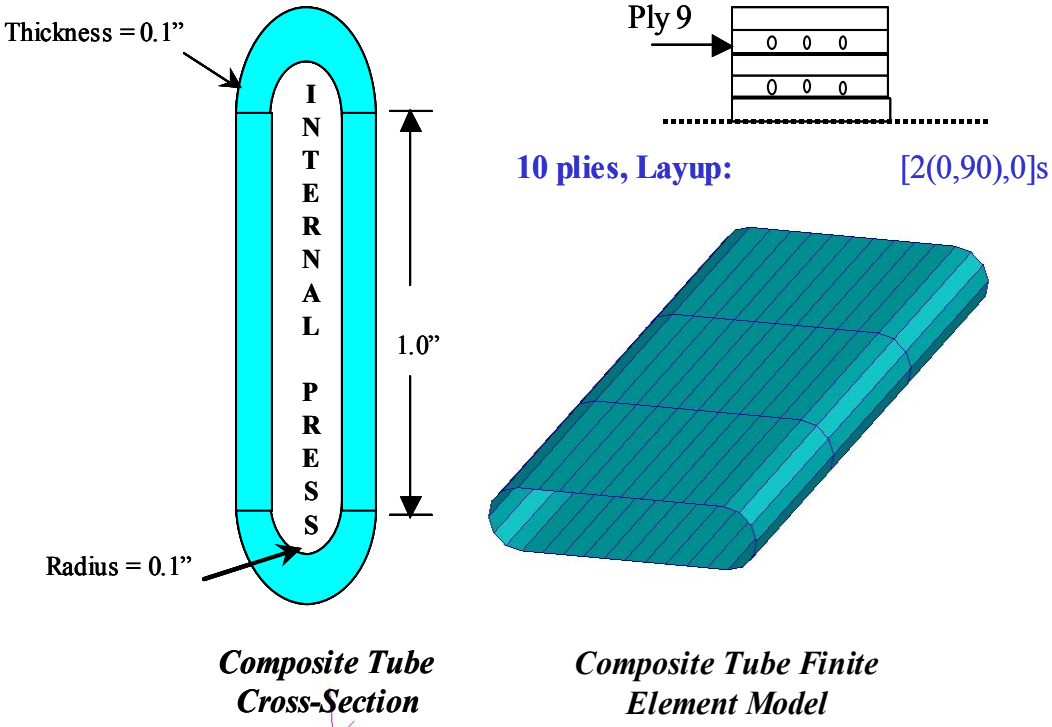

Figure 1. CMC tube cross-section, ply layup and finite element model

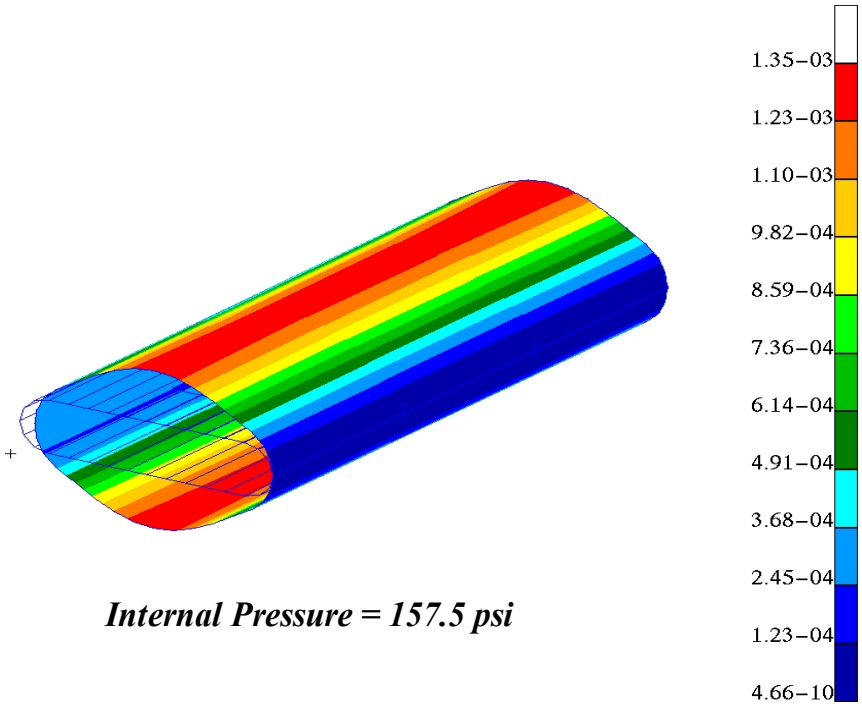

Figure 2. CMC tube deterministic resultant displacements

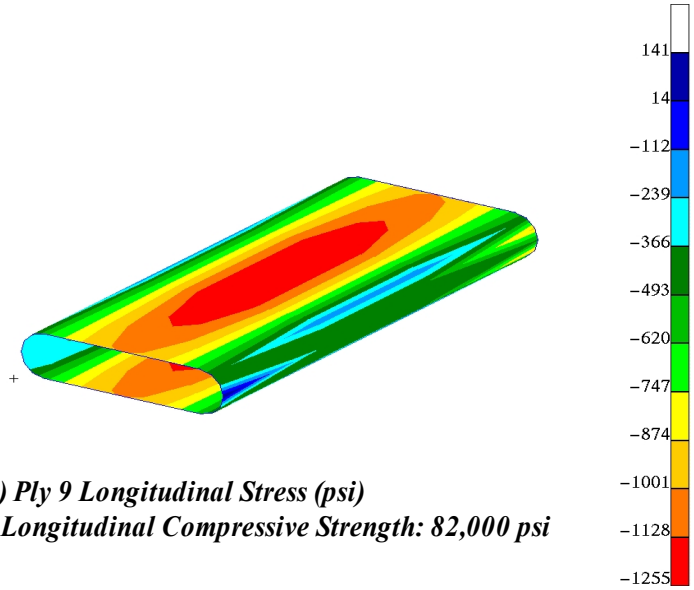

(a) Ply 9 Longitudinal Stress (psi)
Longitudinal Compressive Strength: 82,000 psi

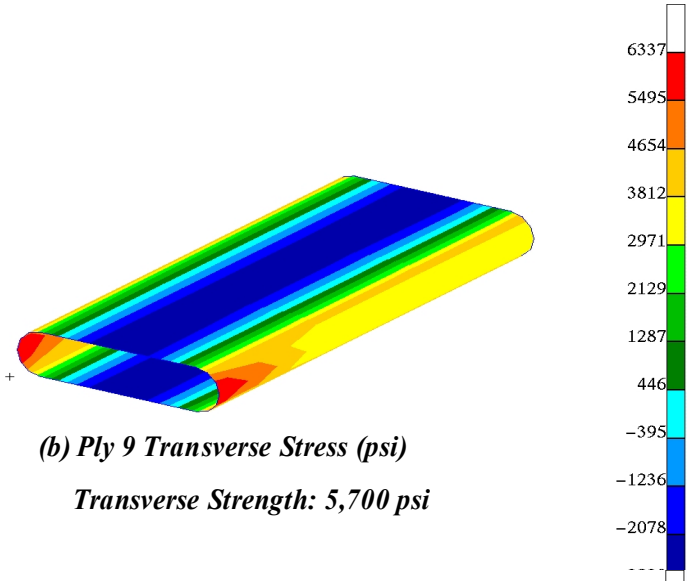

(b) Ply 9 Transverse Stress (psi)
Transverse Strength: 5,700 psi

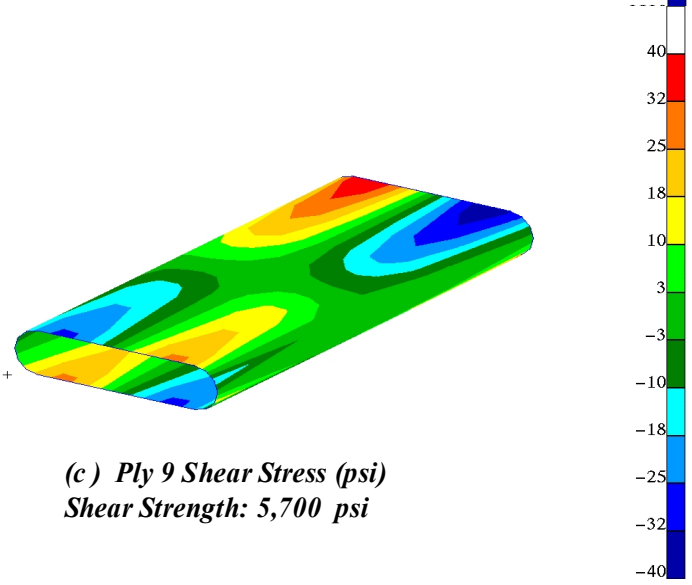

(c) Ply 9 Shear Stress (psi)
Shear Strength: 5,700 psi

Figure 3. CMC tube deterministic ply longitudinal, transverse, and shear stresses

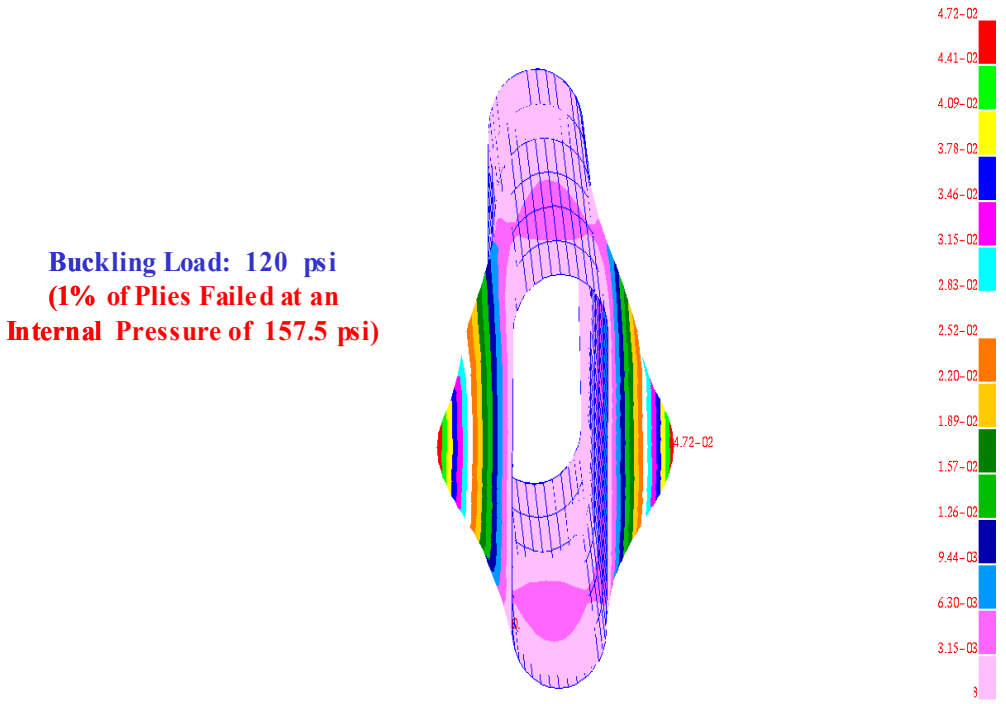

Figure 4. CMC tube deterministic first buckling mode shape

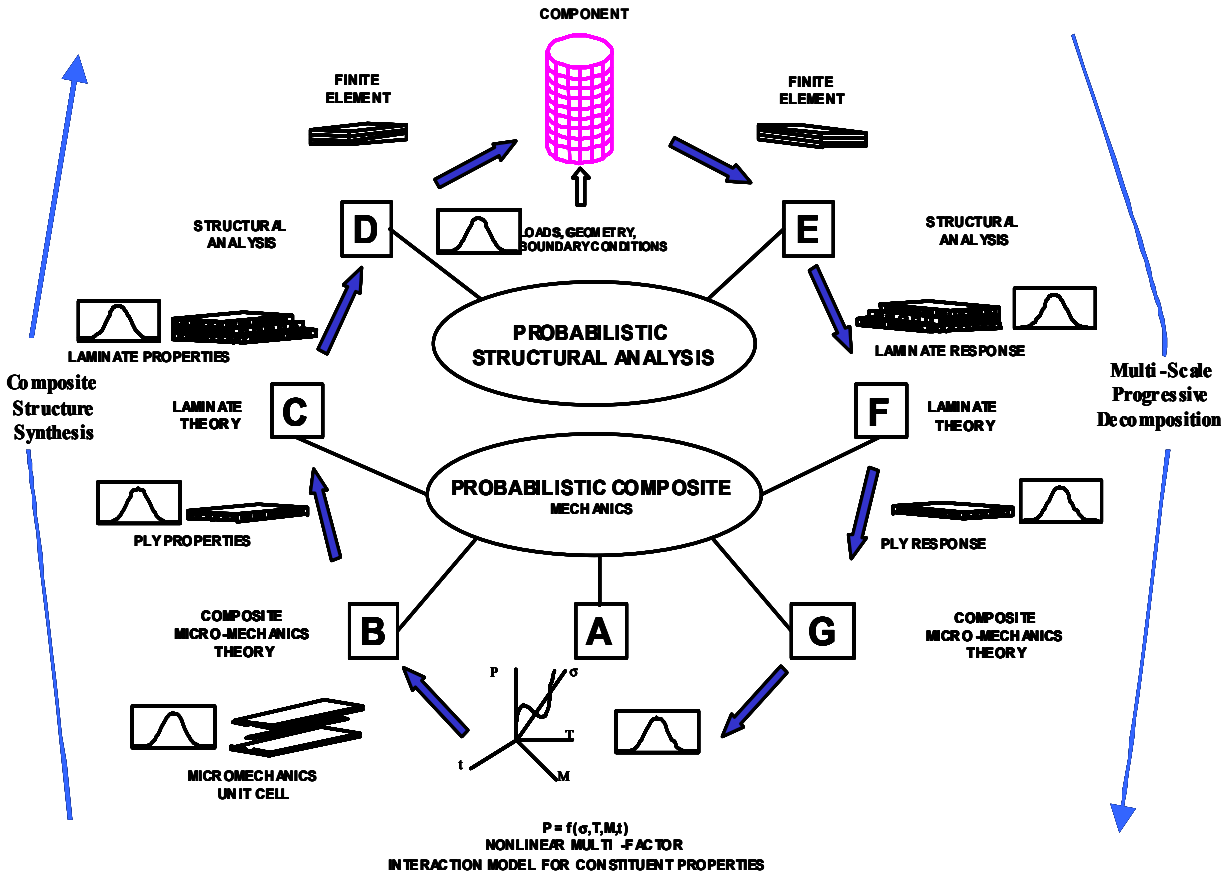

Figure 5. Flow diagram for the probabilistic computational simulation code IPACS

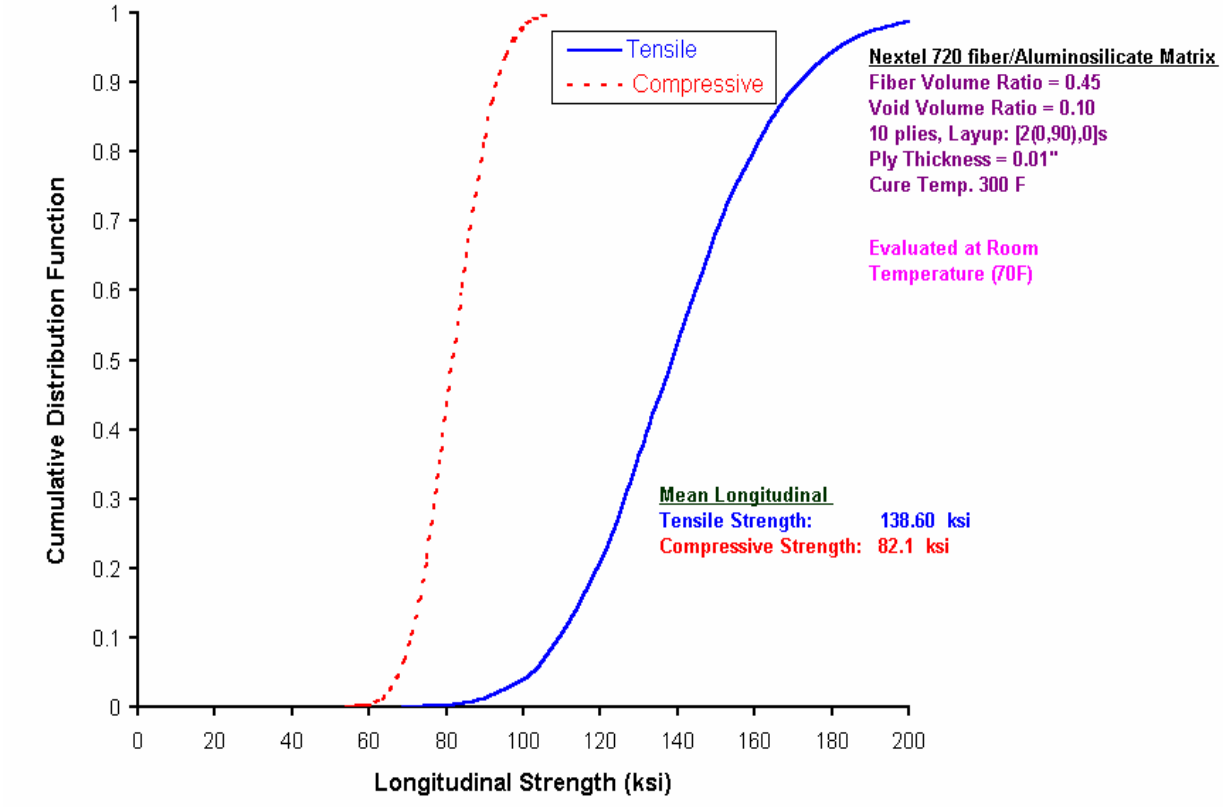

Figure 6. CMC tube - Ply 9 probabilistic longitudinal strength

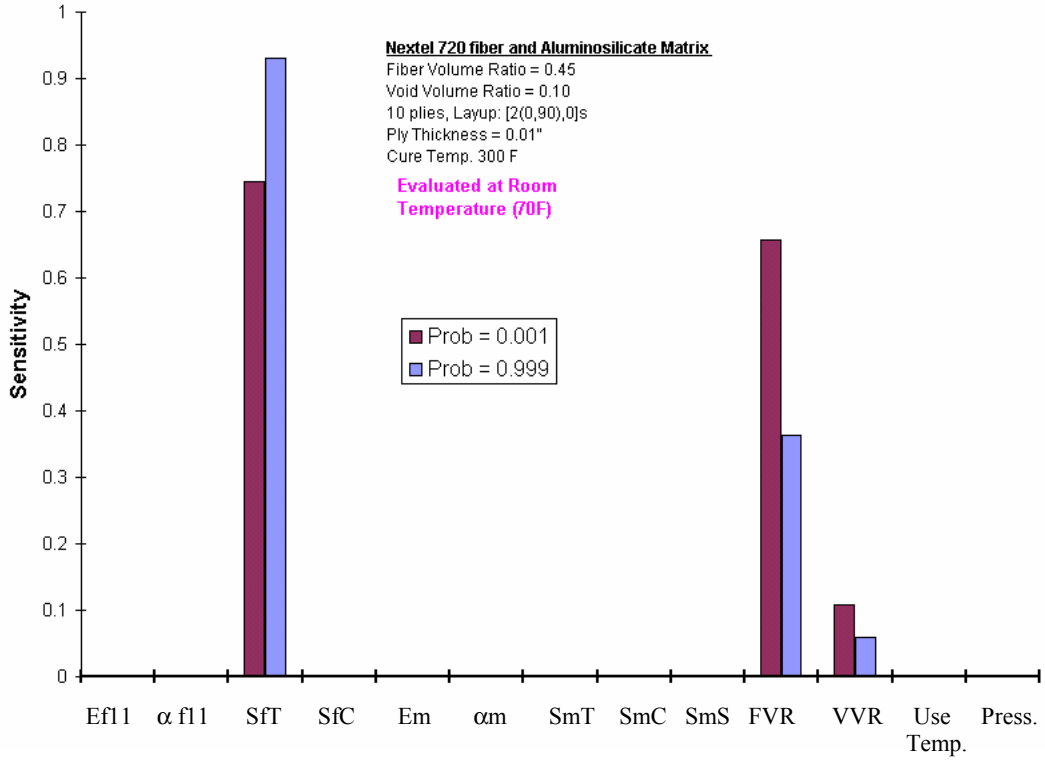

Figure 7. CMC tube - Ply 9 longitudinal tensile strength probabilistic sensitivities

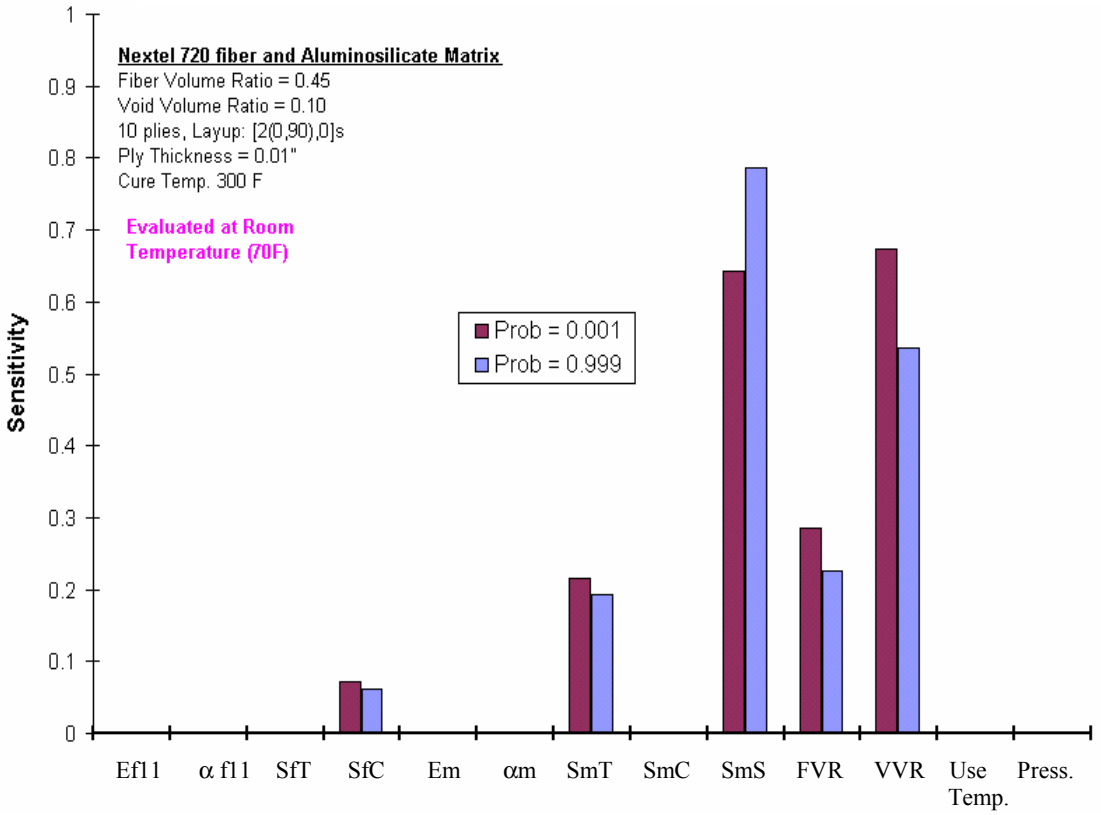

Figure 8. CMC tube - Ply 9 longitudinal compressive strength probabilistic sensitivities

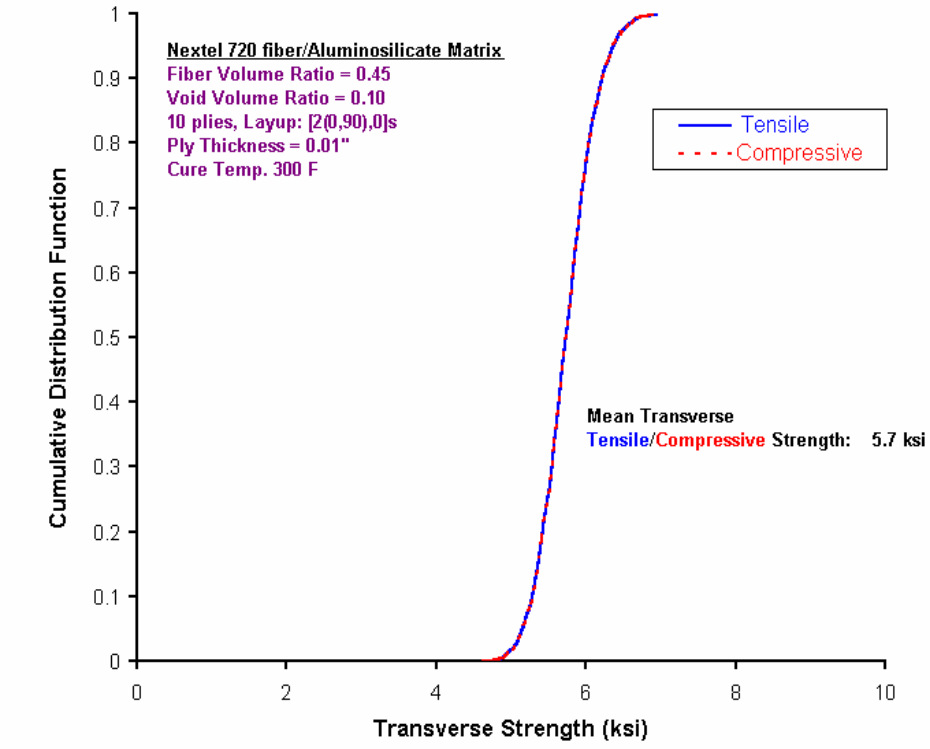

Figure 9. CMC tube - Ply 9 probabilistic transverse strength

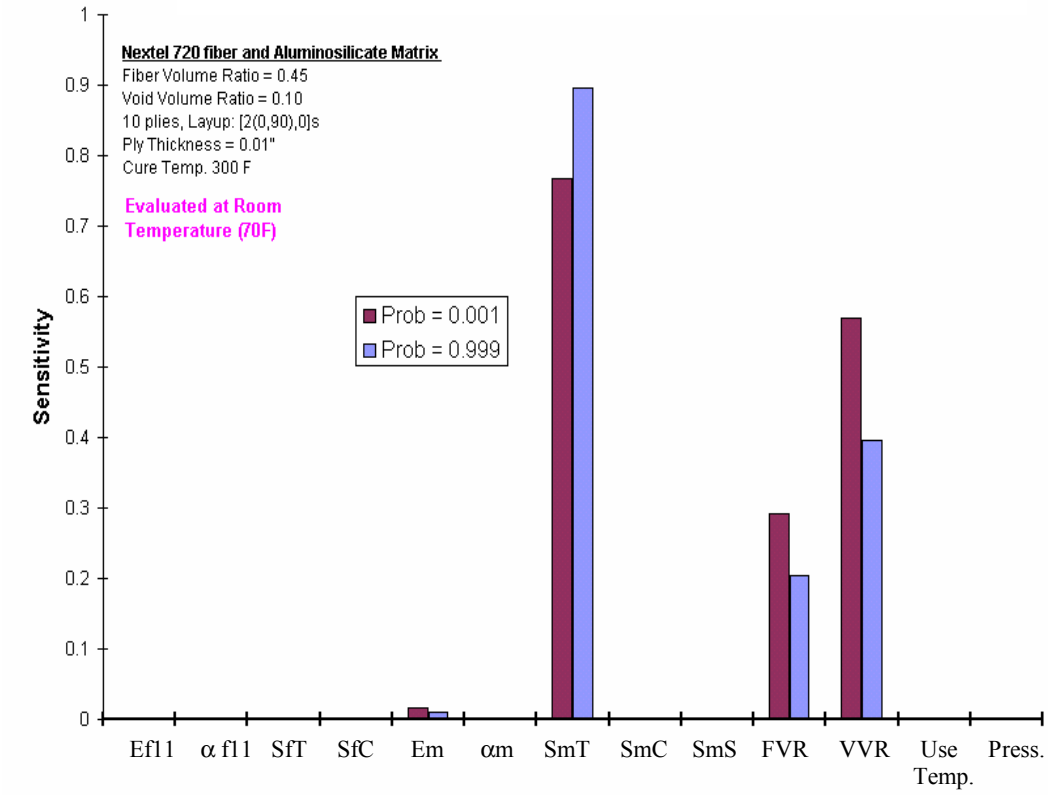

Figure 10. CMC tube - Ply 9 transverse strength probabilistic sensitivities

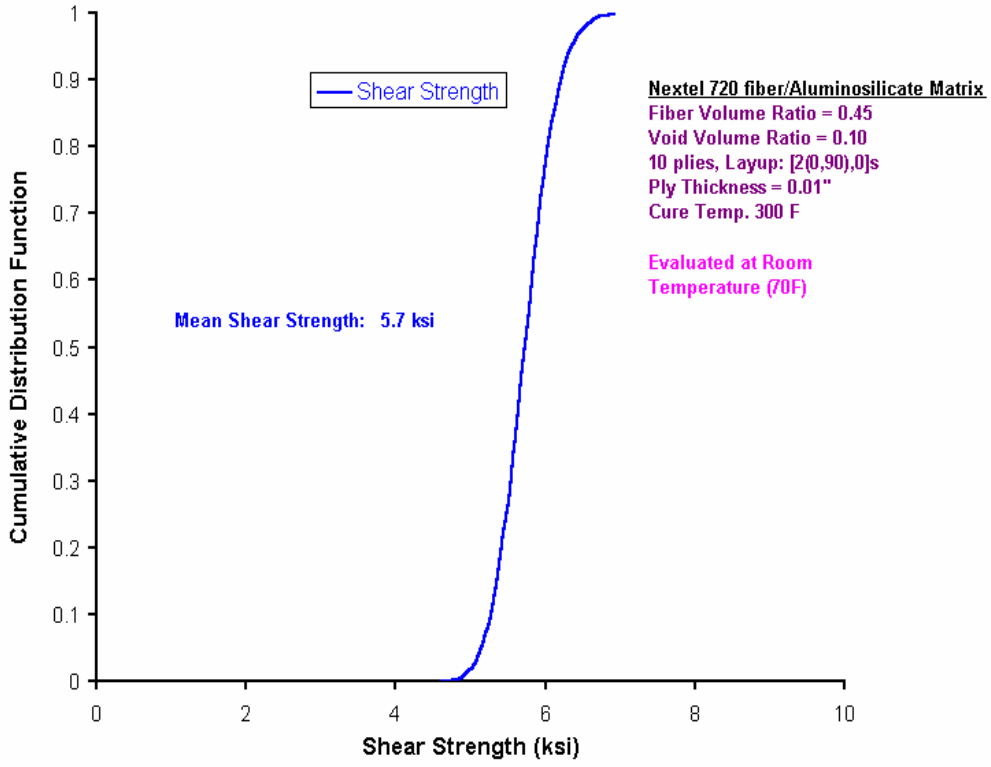

Figure 11. CMC tube - Ply 9 probabilistic shear strength

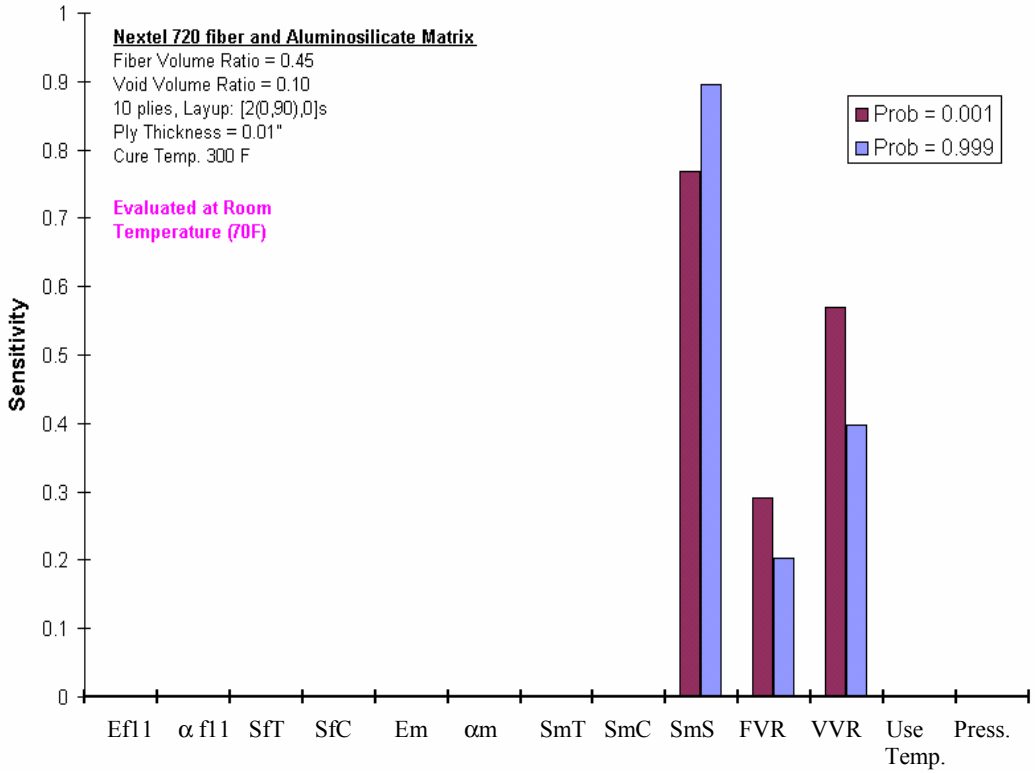

Figure 12. CMC tube - Ply 9 shear strength probabilistic sensitivities

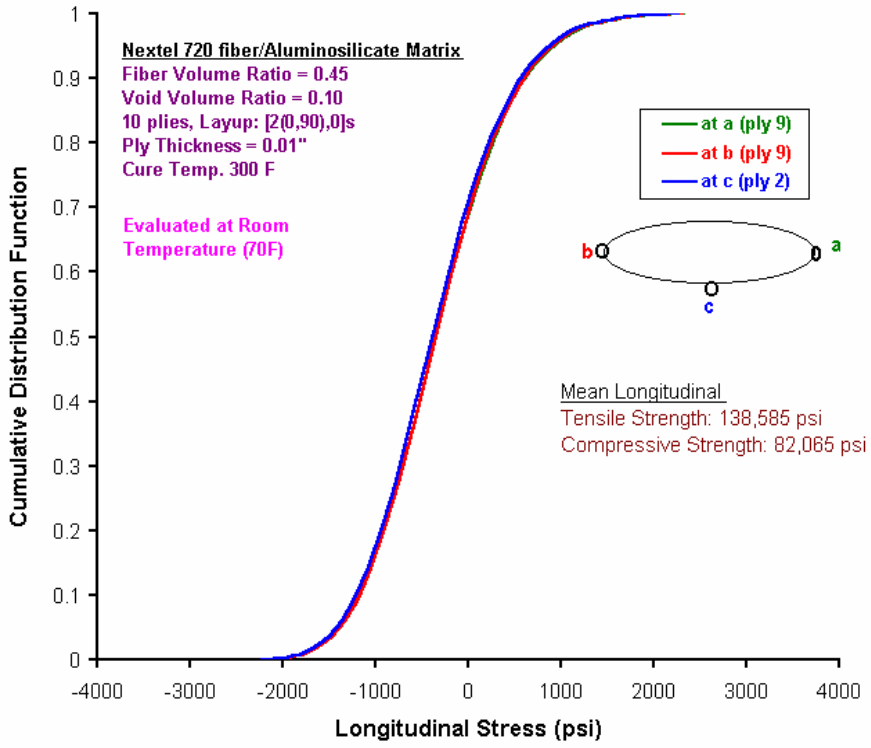

Figure 13. CMC tube - Ply probabilistic longitudinal stress (30 psi pressure)

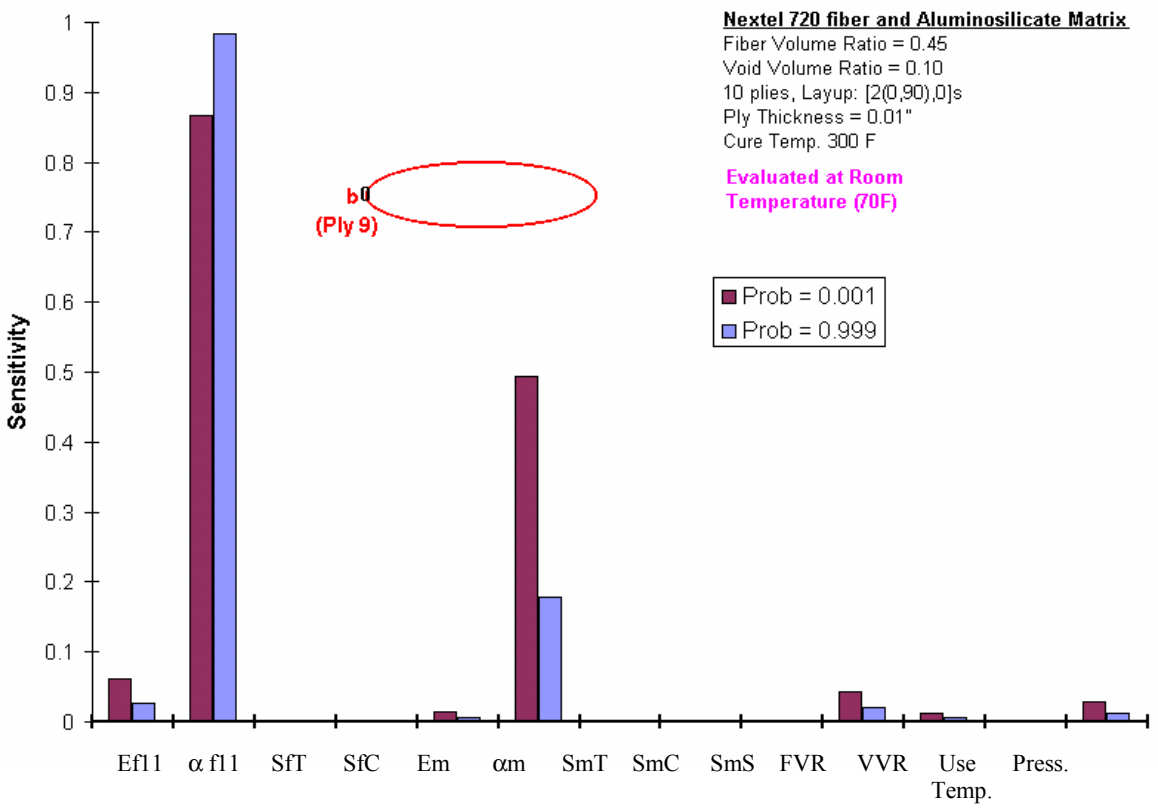

Figure 14. CMC tube - Ply longitudinal stress probabilistic sensitivities (30 psi pressure)

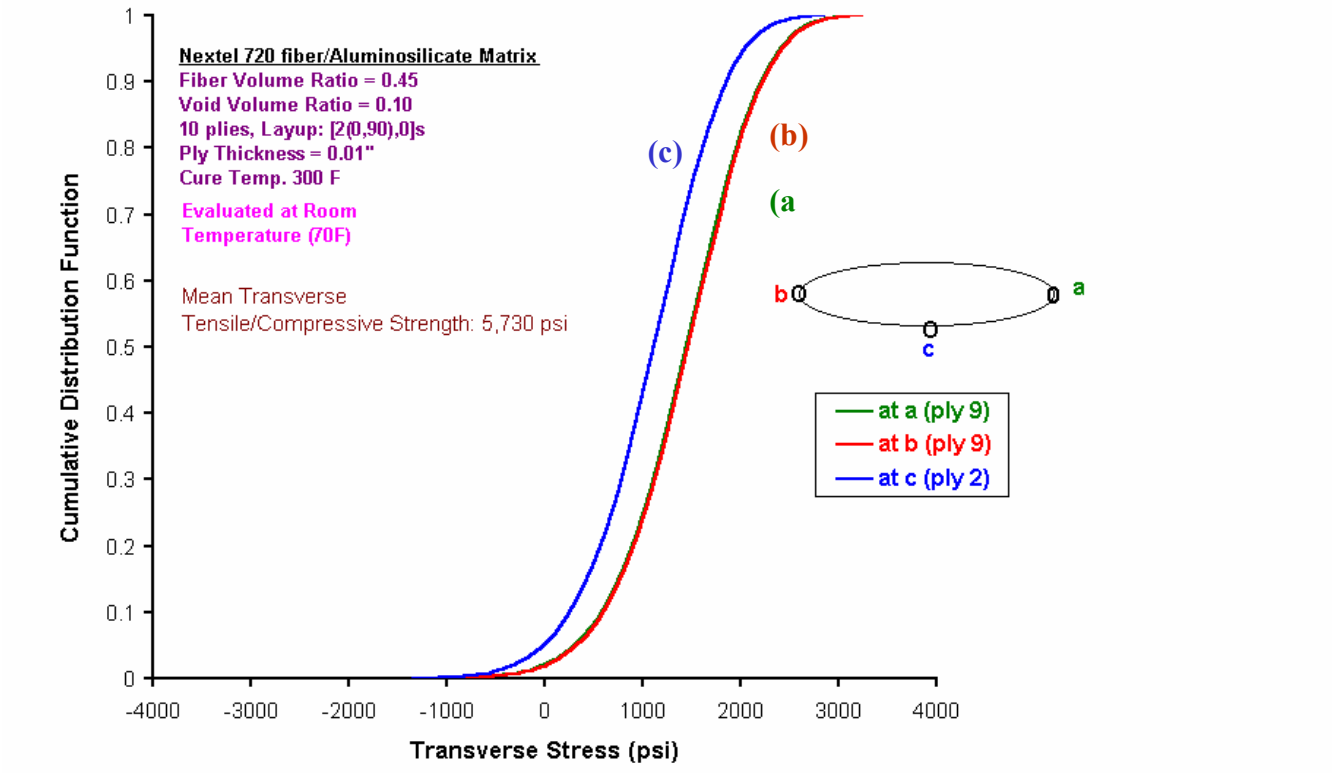

Figure 15. CMC tube - Ply probabilistic transverse stress (30 psi pressure)

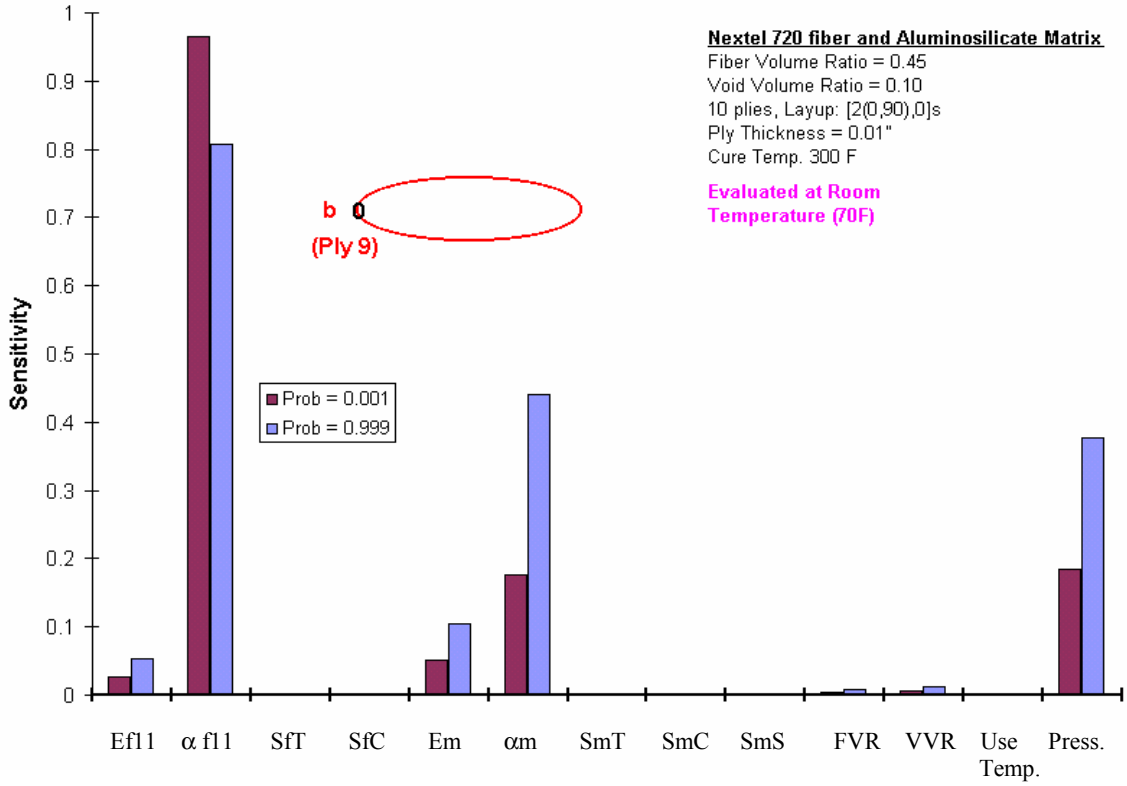

Figure 16. CMC tube - Ply transverse stress probabilistic sensitivities (30 psi pressure)

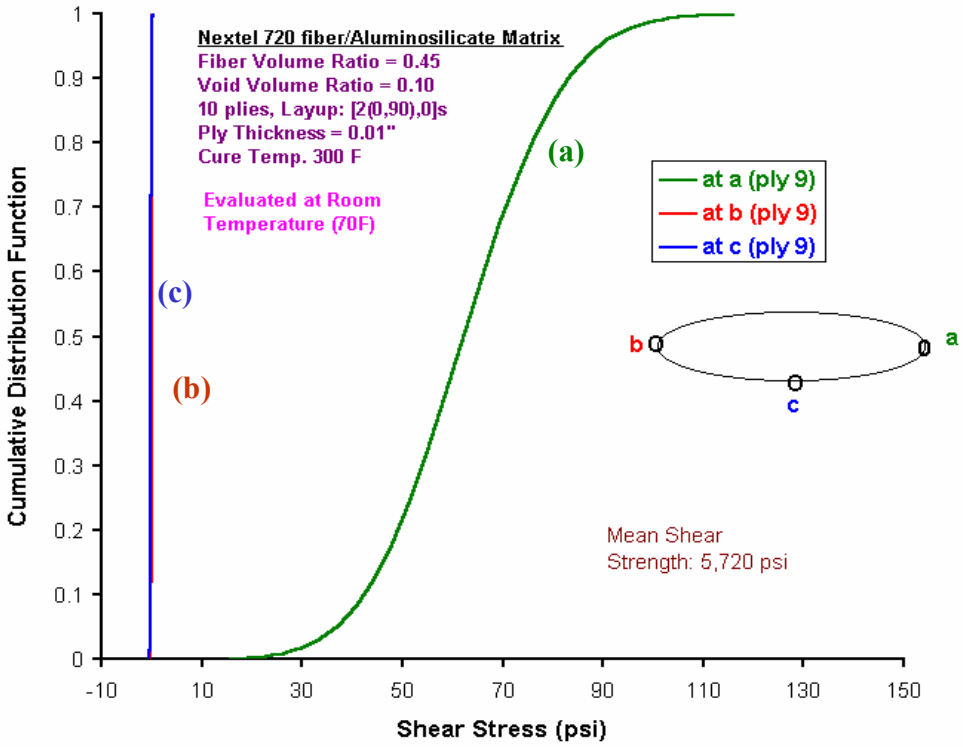

Figure 17. CMC tube - Ply probabilistic shear stress (30 psi pressure)

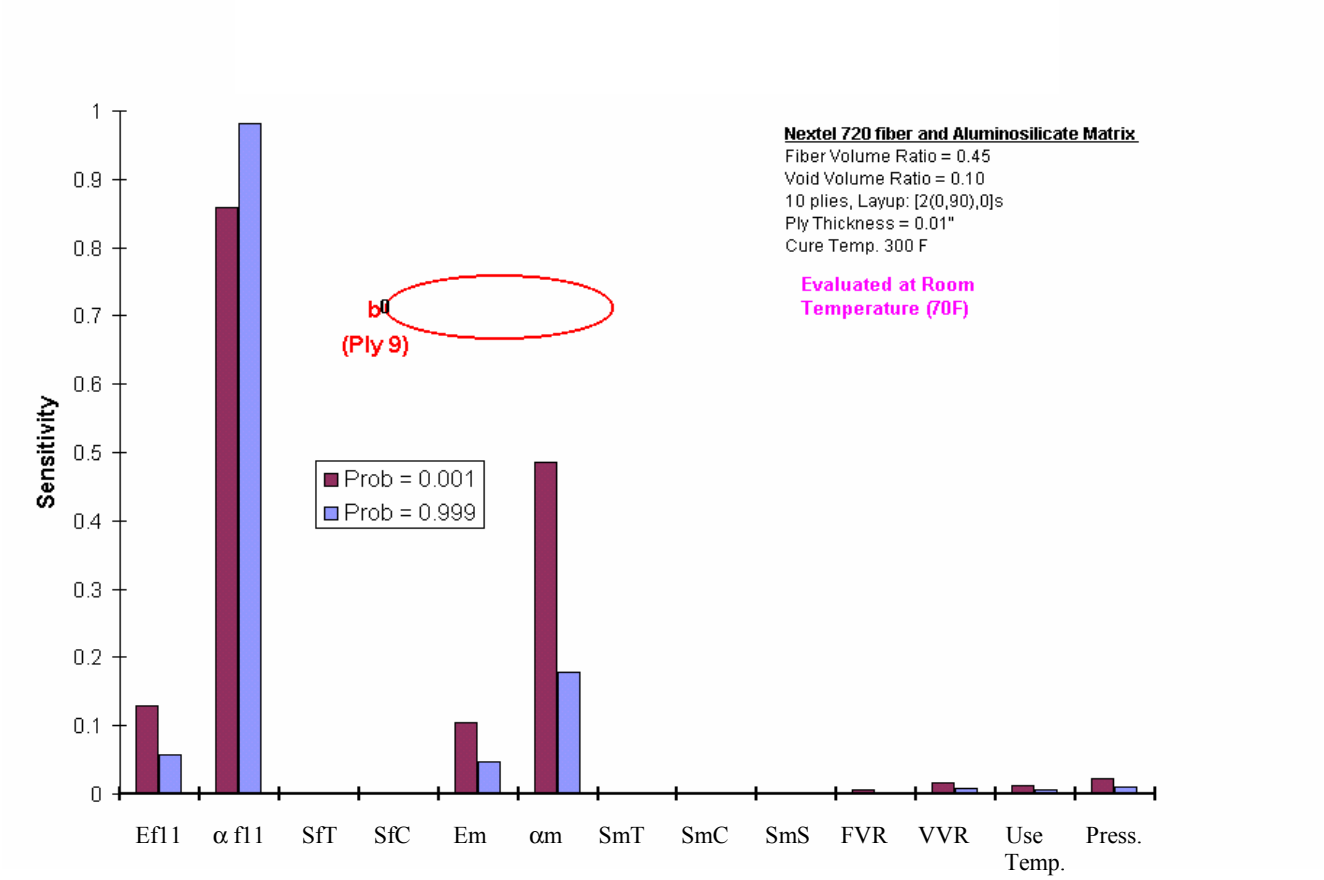

Figure 18. CMC tube - Ply shear stress probabilistic sensitivities (30 psi pressure)

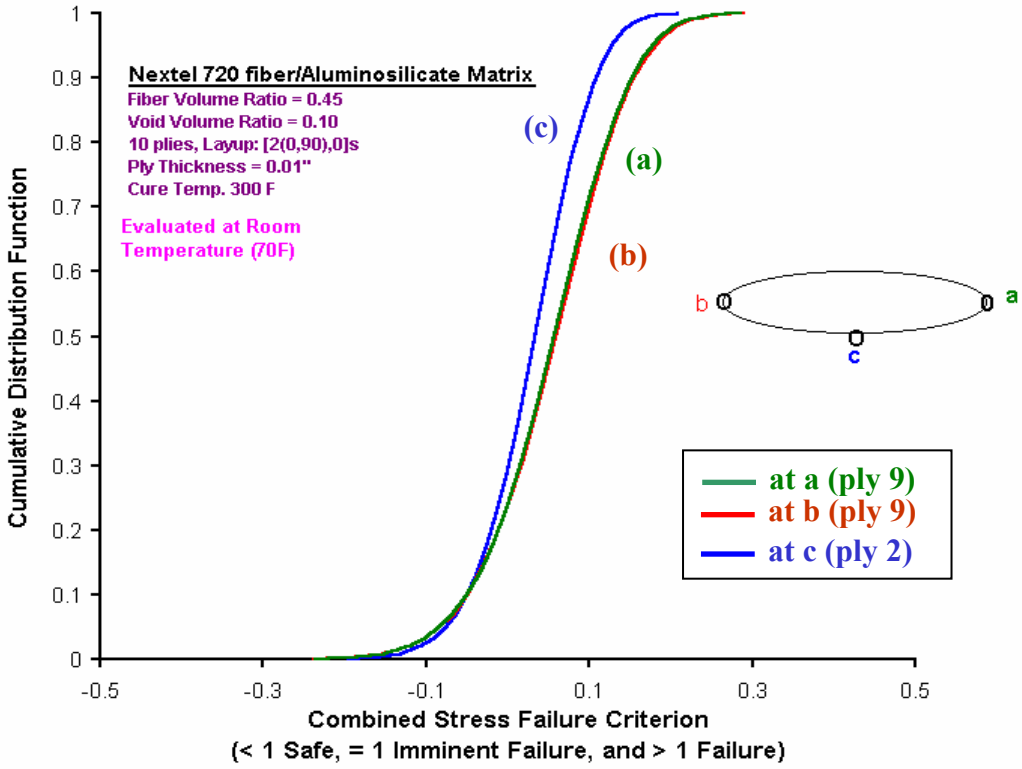

Figure 19. Probabilistic ply combined stress failure criterion (30 psi pressure)

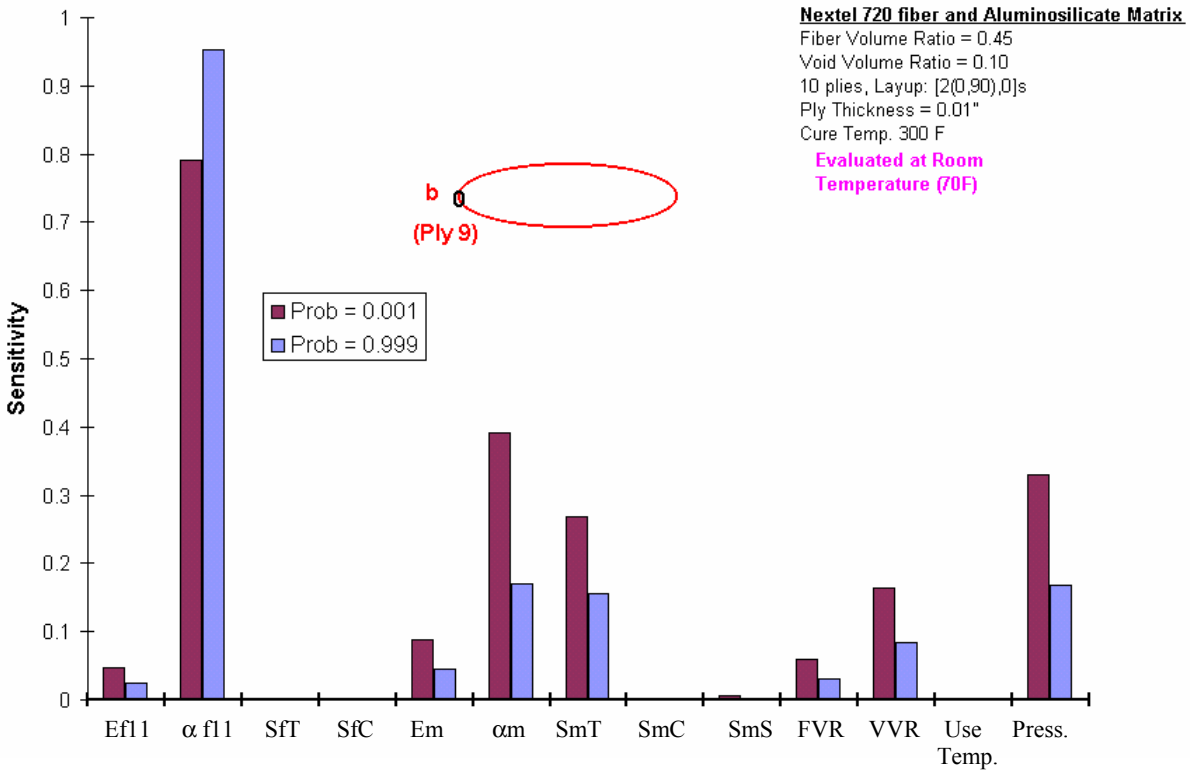

Figure 20. Probabilistic sensitivities for ply combined stress failure criterion (30 psi pressure)

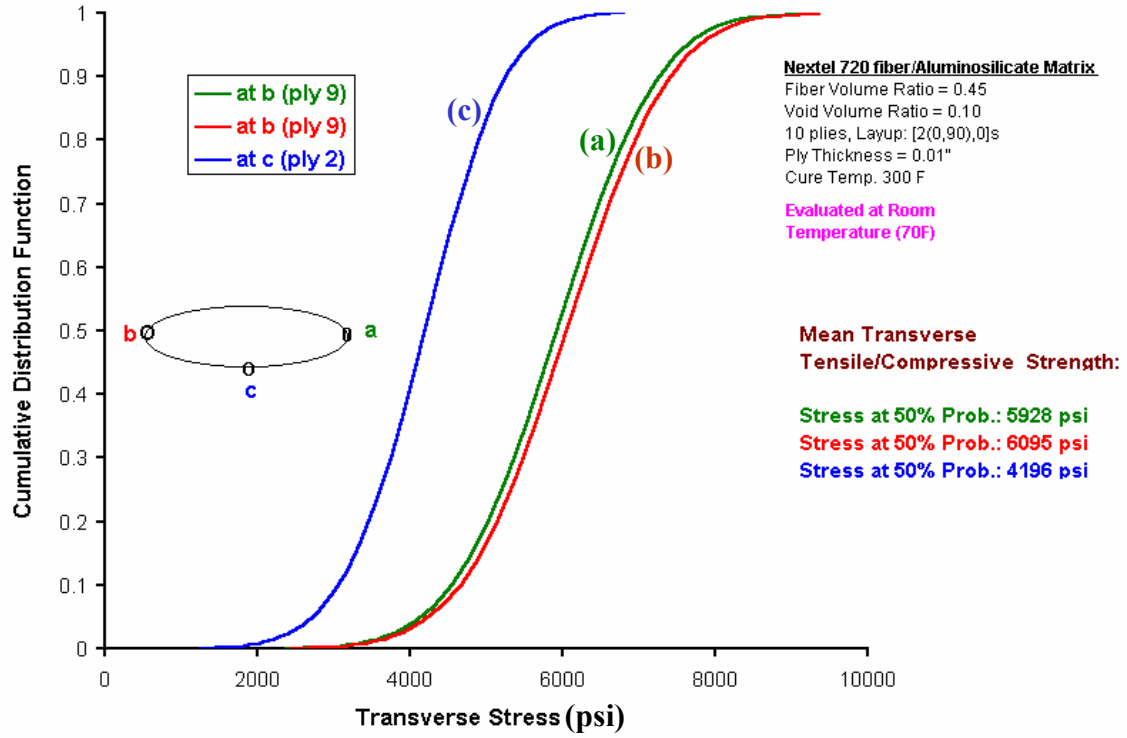

Figure 21. CMC tube - Probabilistic ply transverse stress (157.5 psi pressure)

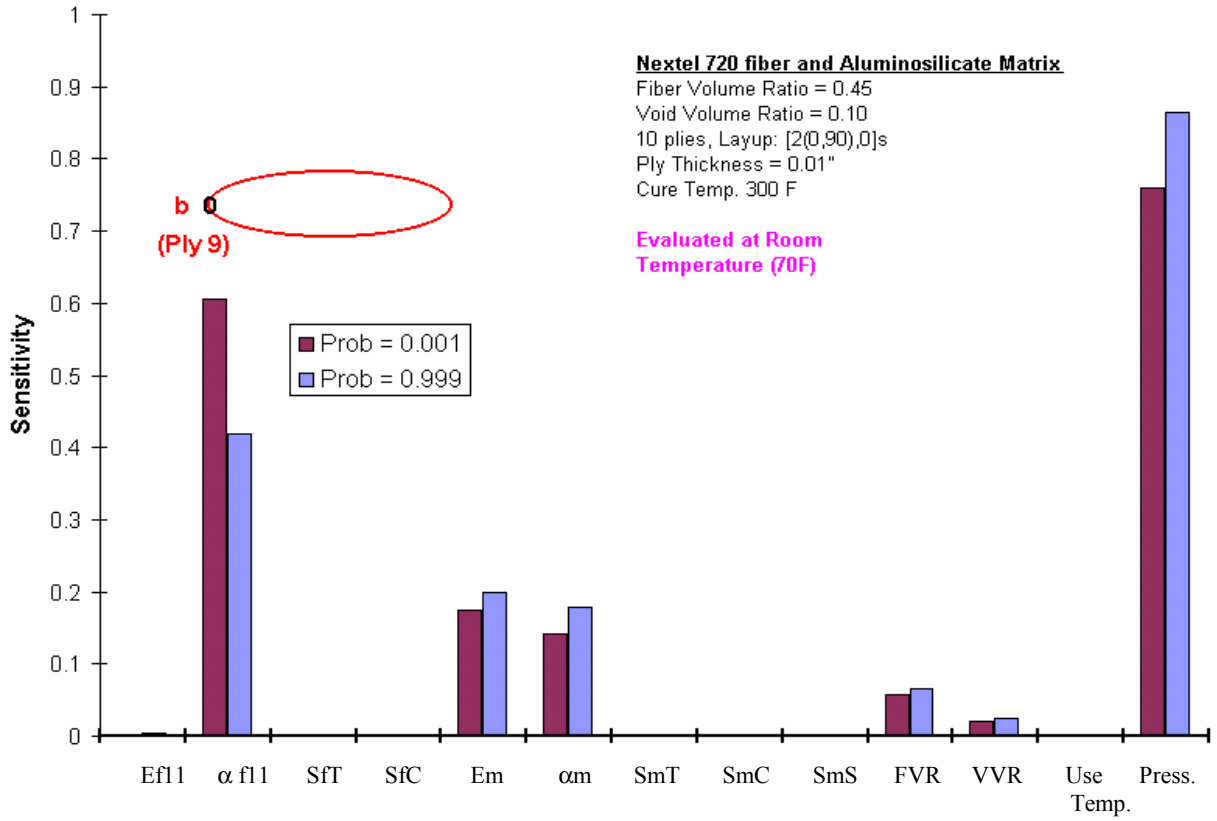

Figure 22. Probabilistic sensitivities for ply transverse stress (157.5 psi pressure)

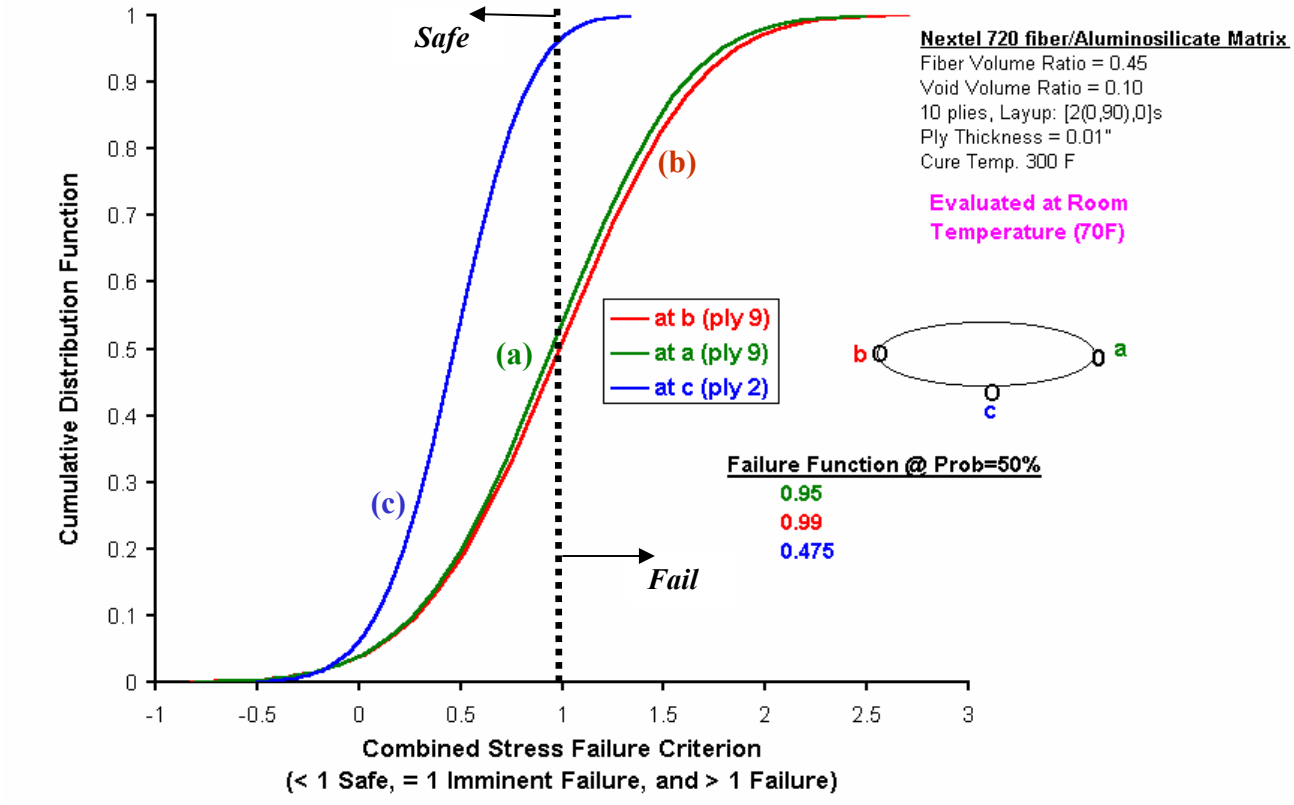

Figure 23-a. Probabilistic ply combined stress failure criterion (157.5 psi pressure and 70 °F)

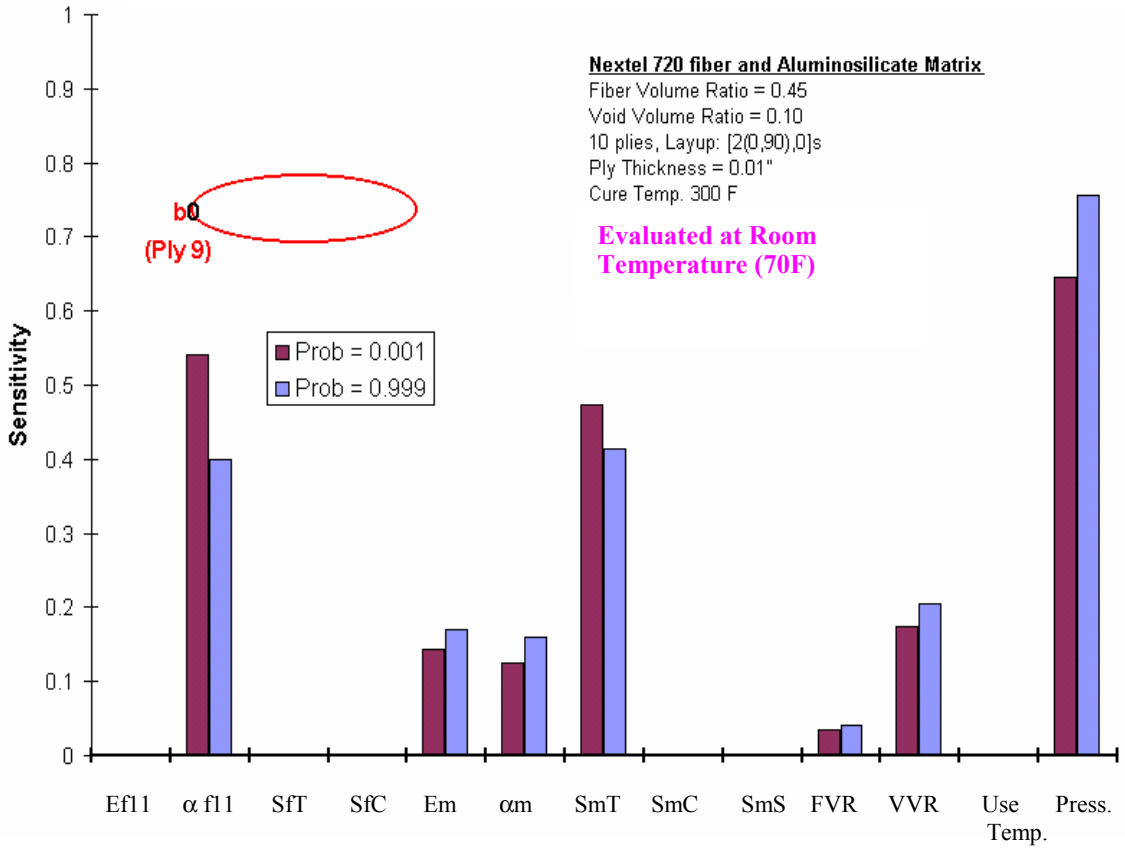

Figure 23-b. Probabilistic sensitivities for ply combined stress failure criterion (157.5 psi pressure and 70 ºF Temp)

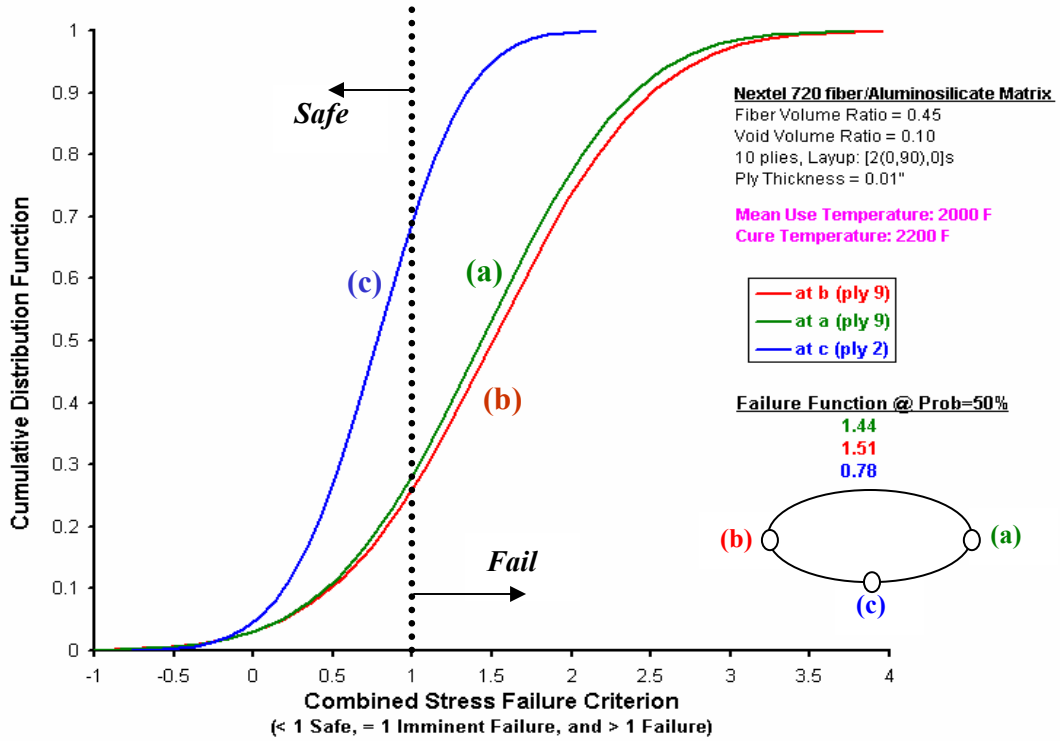

Figure 24-a. Probabilistic ply combined stress failure criterion (157.5 psi pressure and 2000 °F)

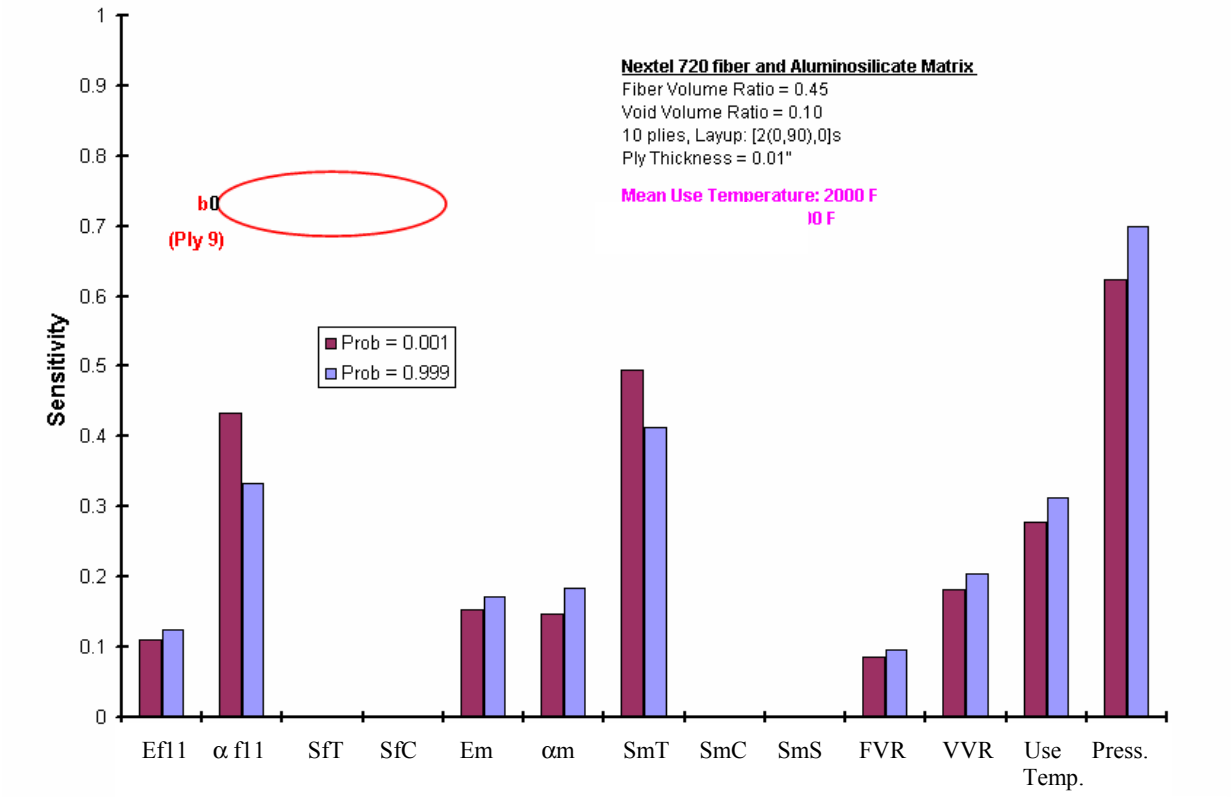

Figure 24-b. Probabilistic sensitivities for ply combined stress failure criterion (157.5 psi pressure and 2000 ºF Temp)

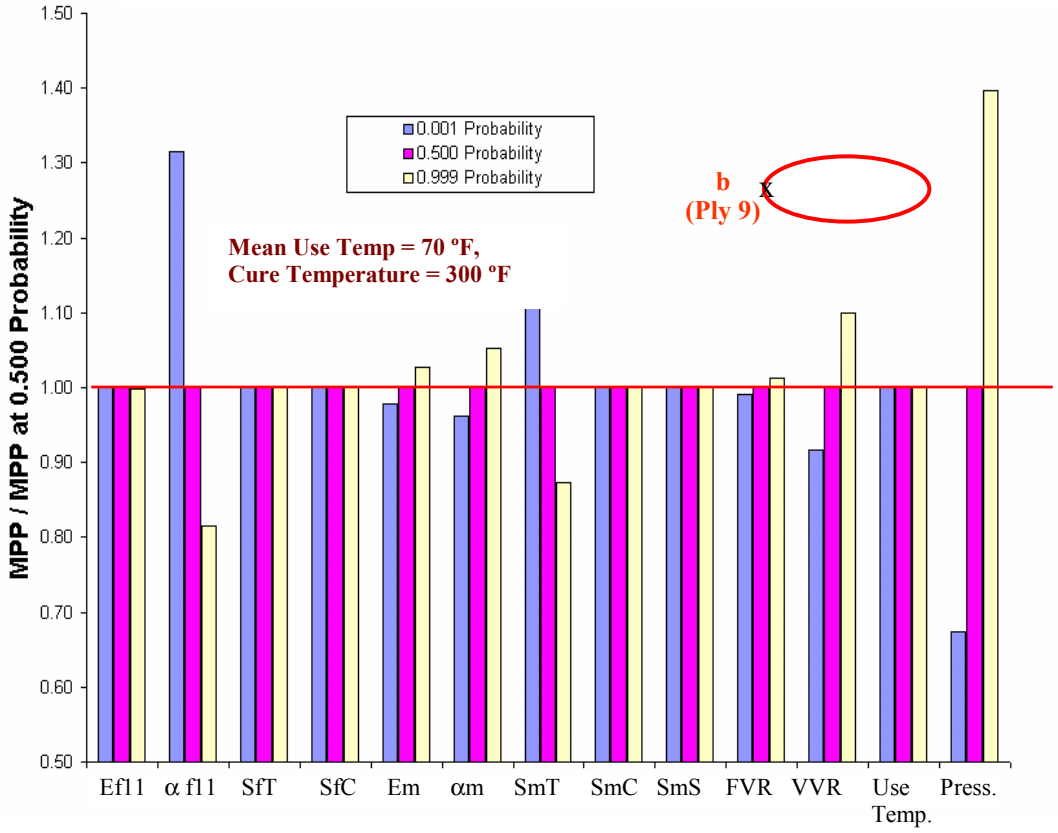

Figure 25. Most probable design for ply 9 combined stress failure criterion (157.5 psi pressure)

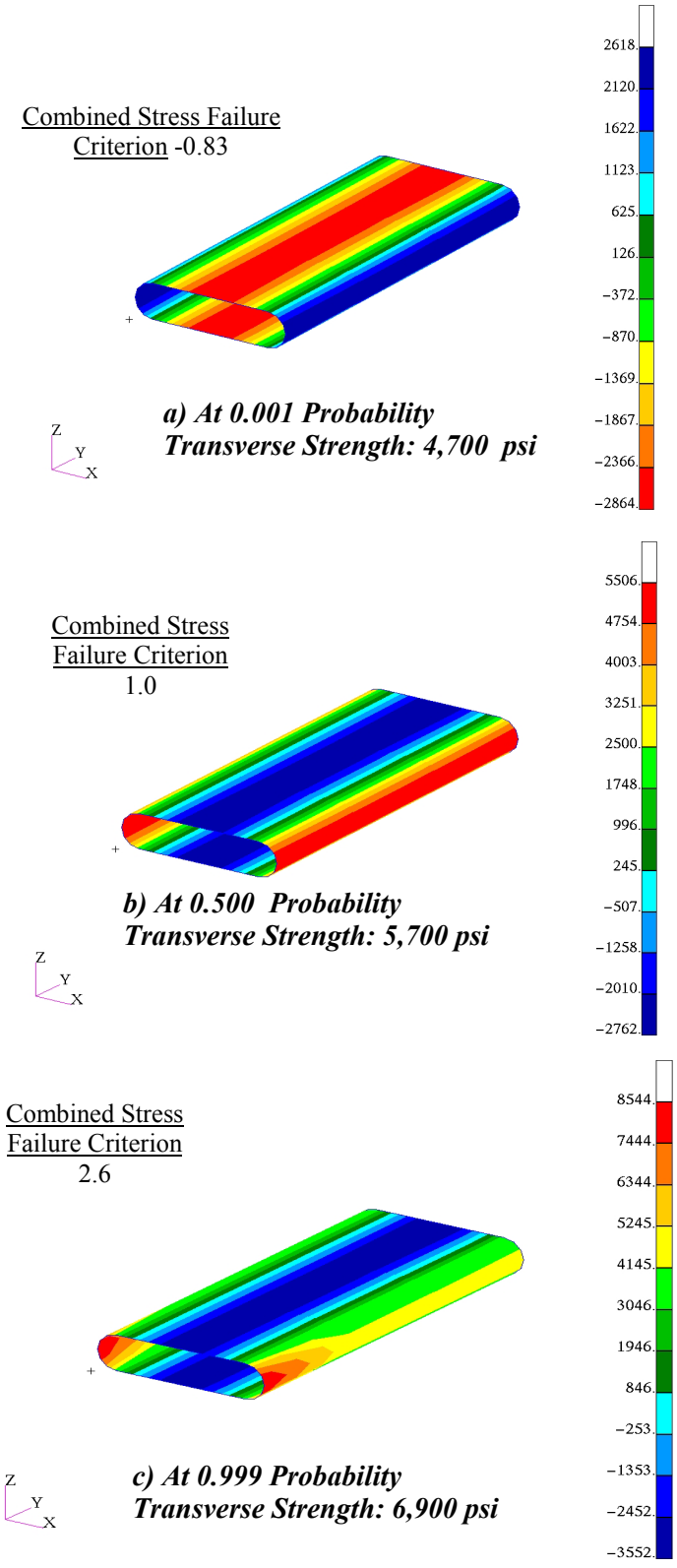

Figure 26. Ply 9 transverse stress based on a) 0.001, b) 0.500 and c) 0.999 probabilistic design of combined stress failure criterion

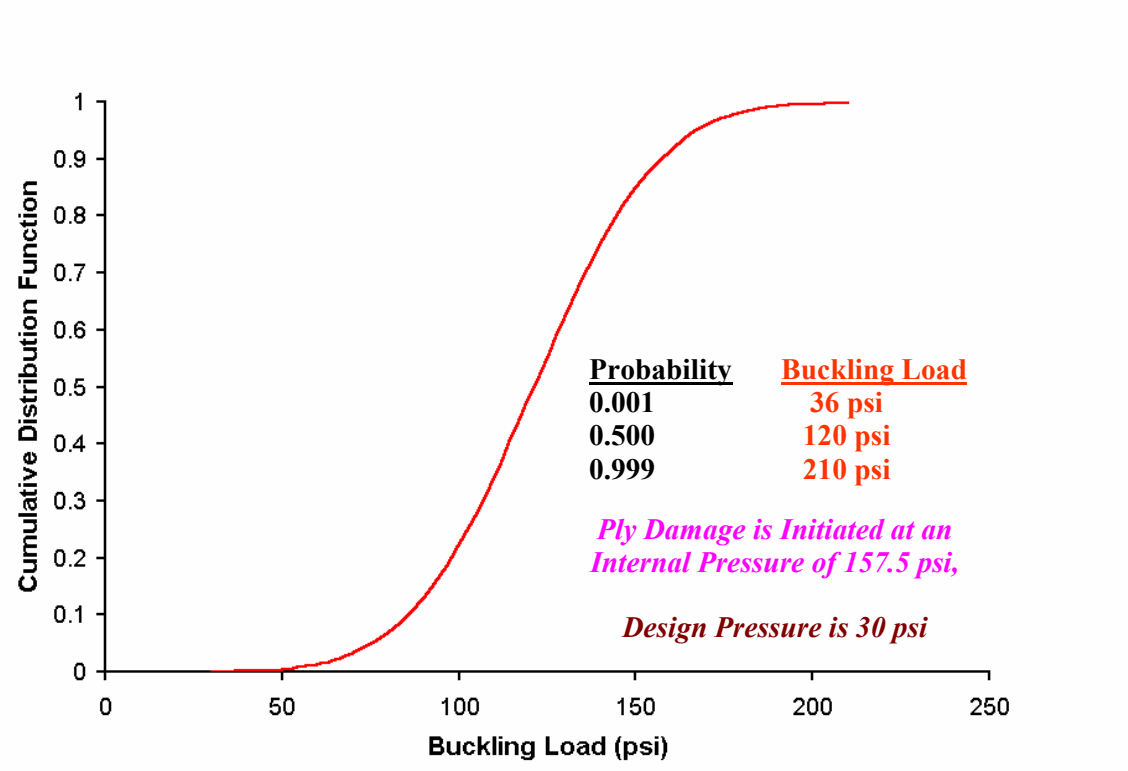

Figure 27. Probabilistic evaluation of buckling load (internally pressurized CMC tube)

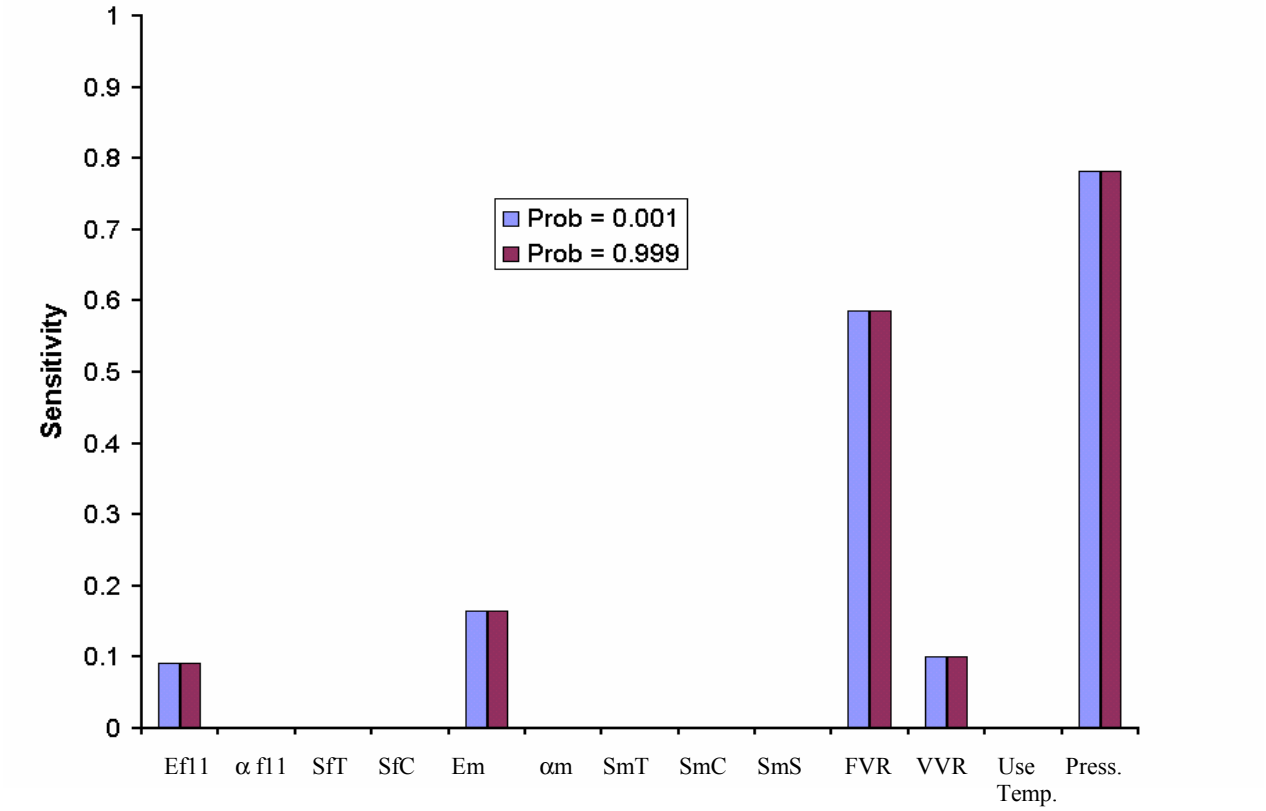

Figure 28. Buckling load probabilistic sensitivities (internally pressurized CMC tube)

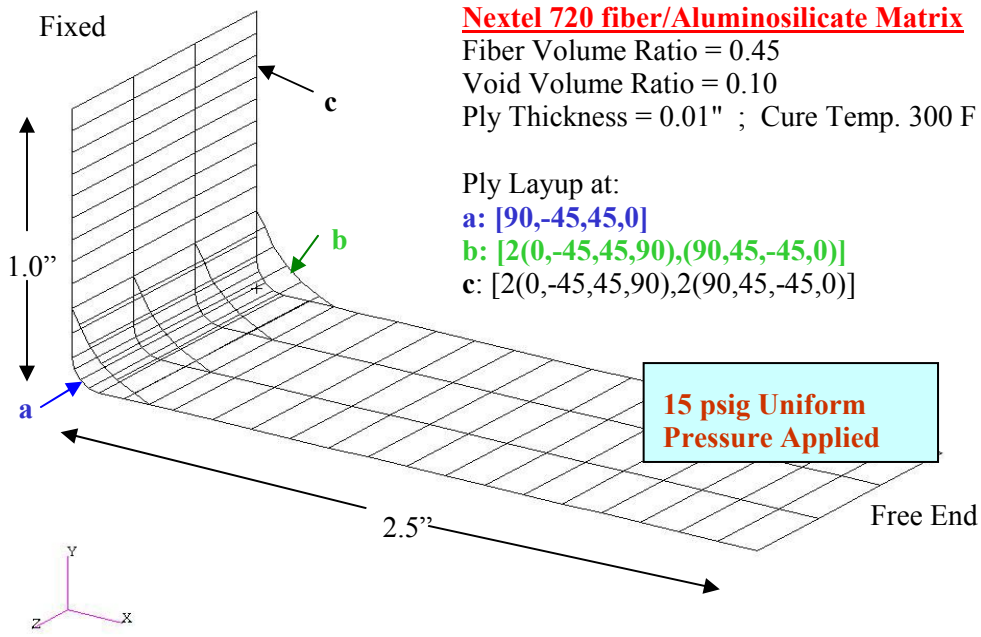

Figure 29. CMC flange model description and material selection

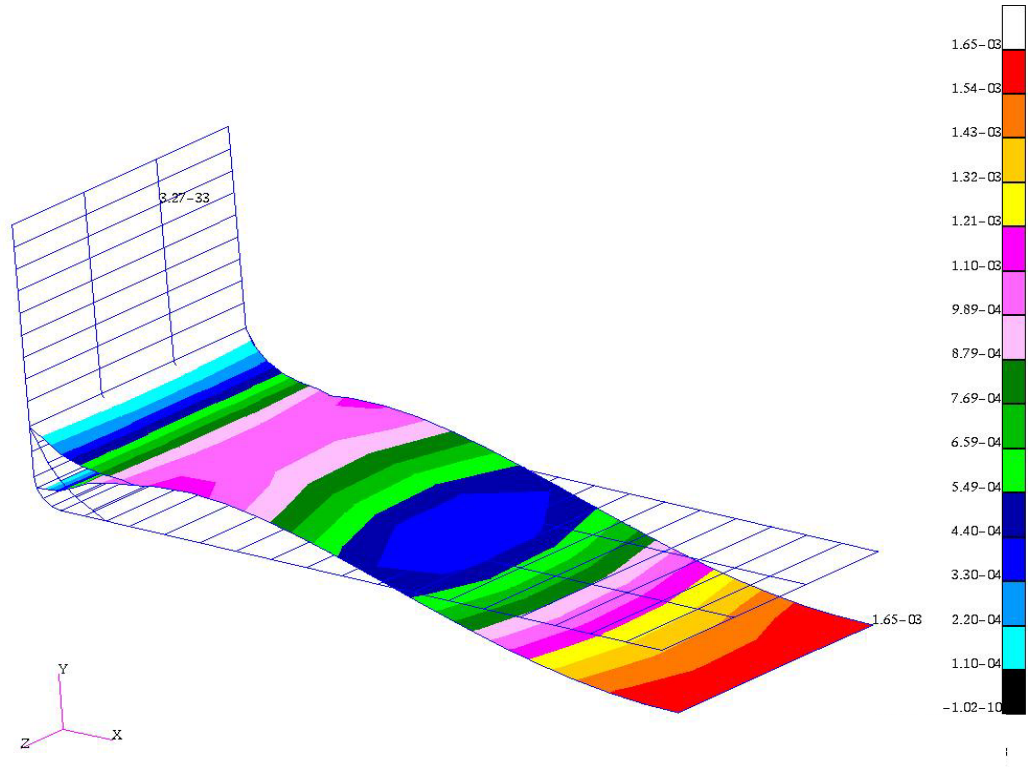

Figure 30. CMC flange deterministic resultant displacements

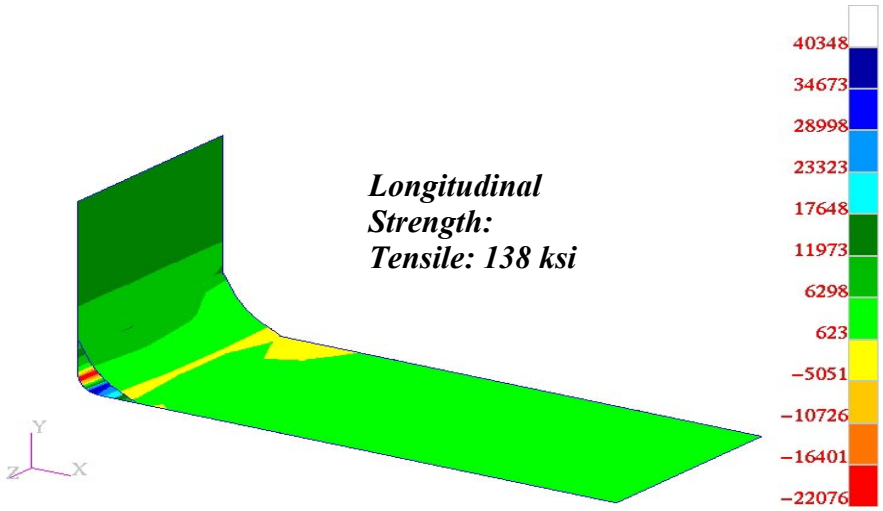

a) Ply 1 longitudinal stress (psi)

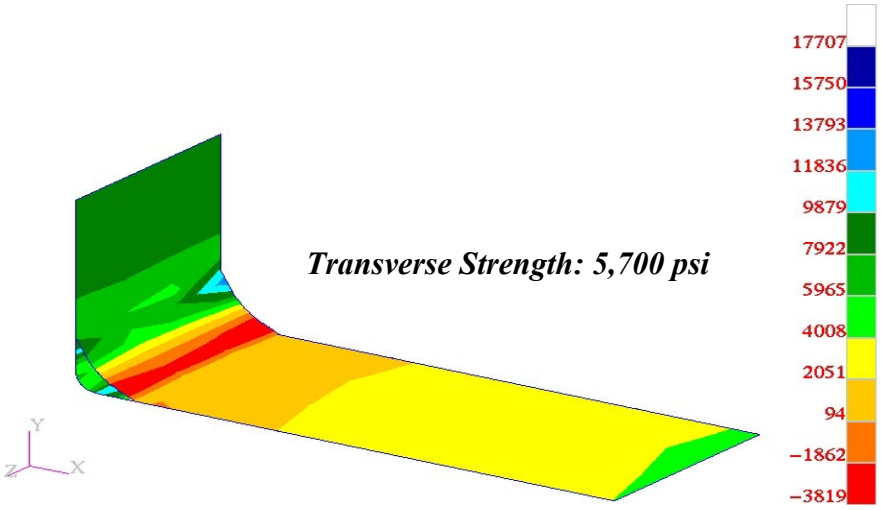

b) Ply 1 transverse stress (psi)

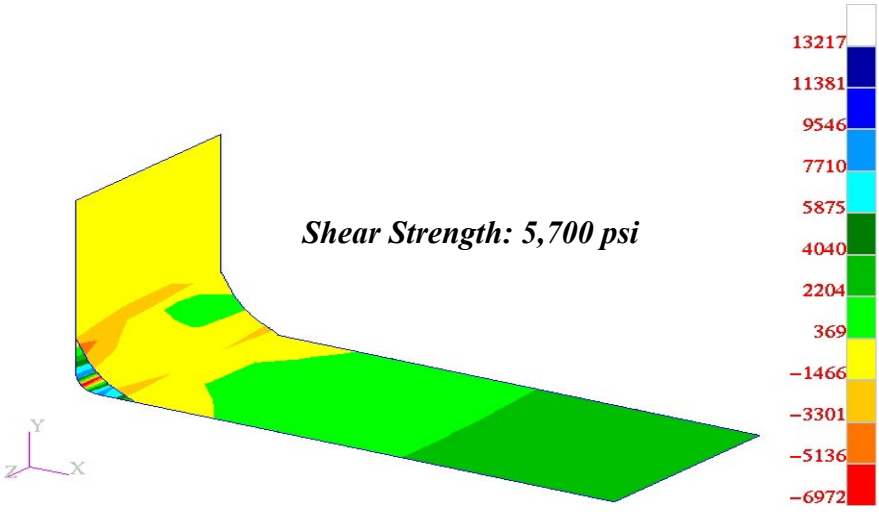

c) Ply 1 shear stress (psi)

Figure 31. CMC flange deterministic bottom ply

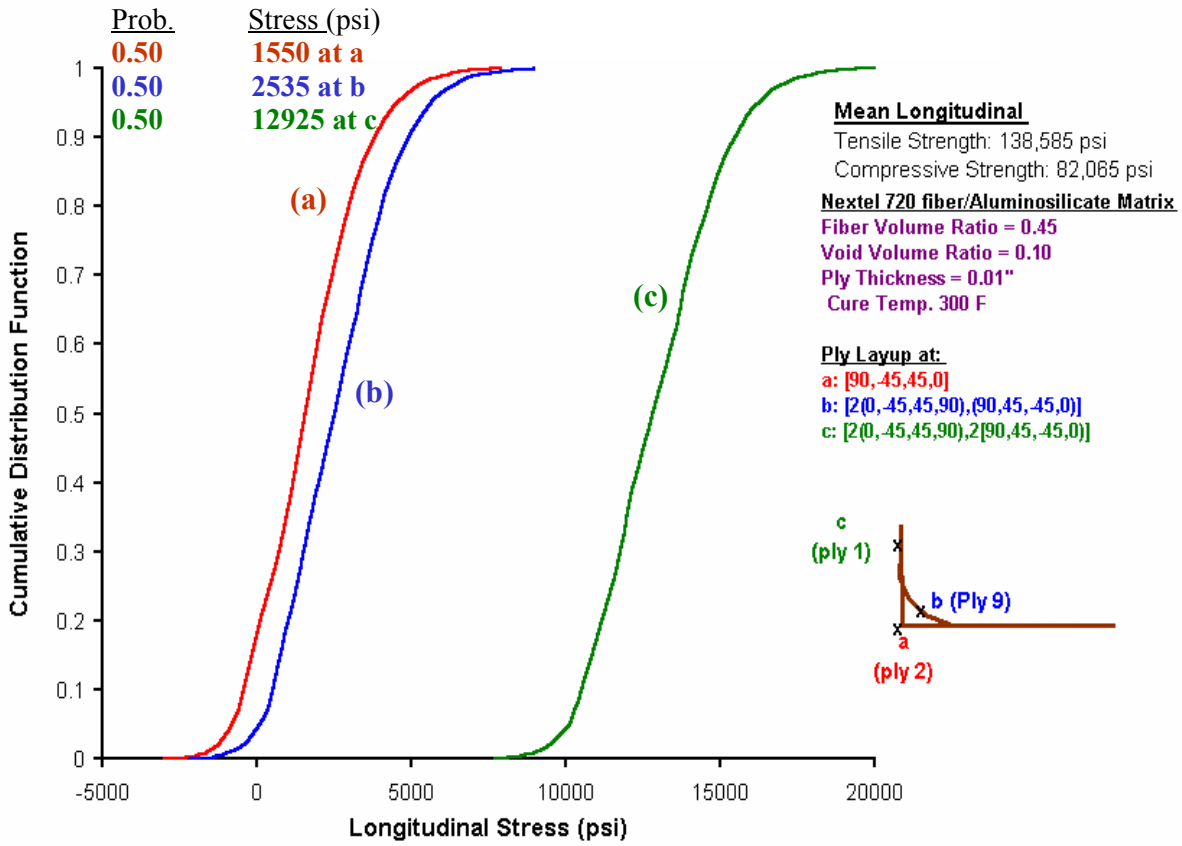

Figure 32. CMC flange – Probabilistic ply longitudinal stress (15 psi pressure)

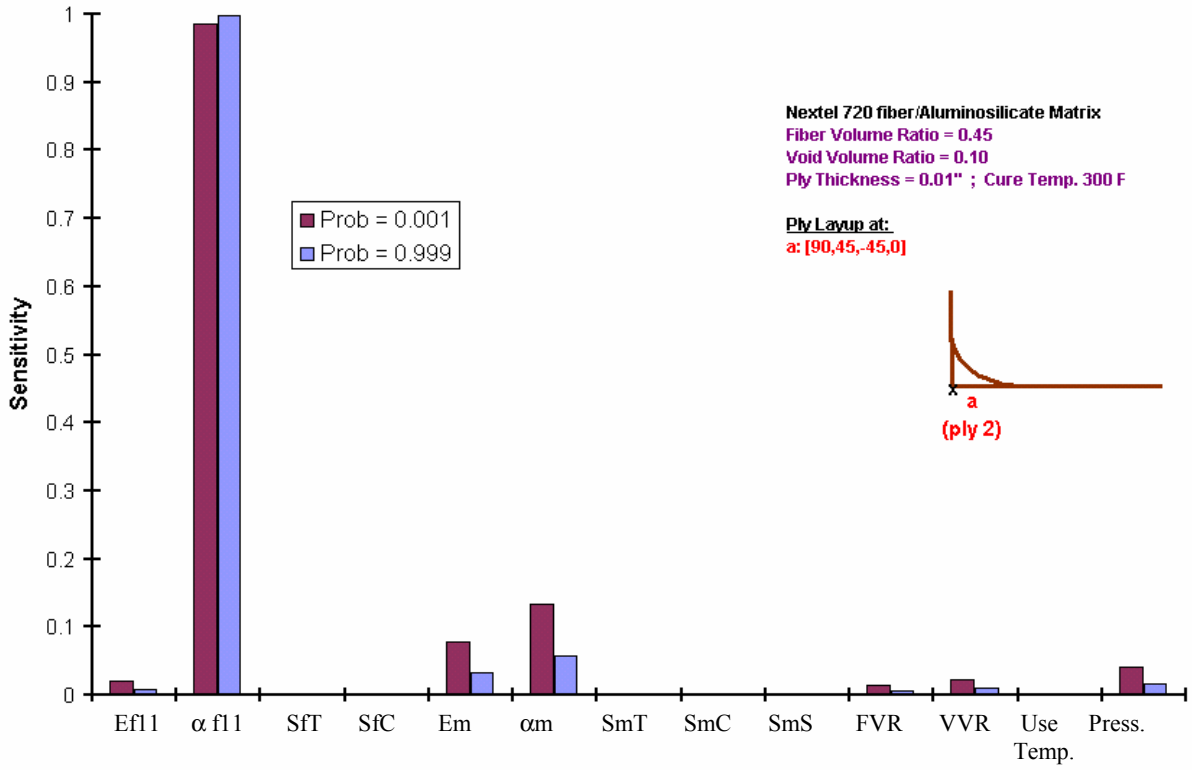

Figure 33. Probabilistic sensitivities for ply longitudinal stress (15 psi pressure)

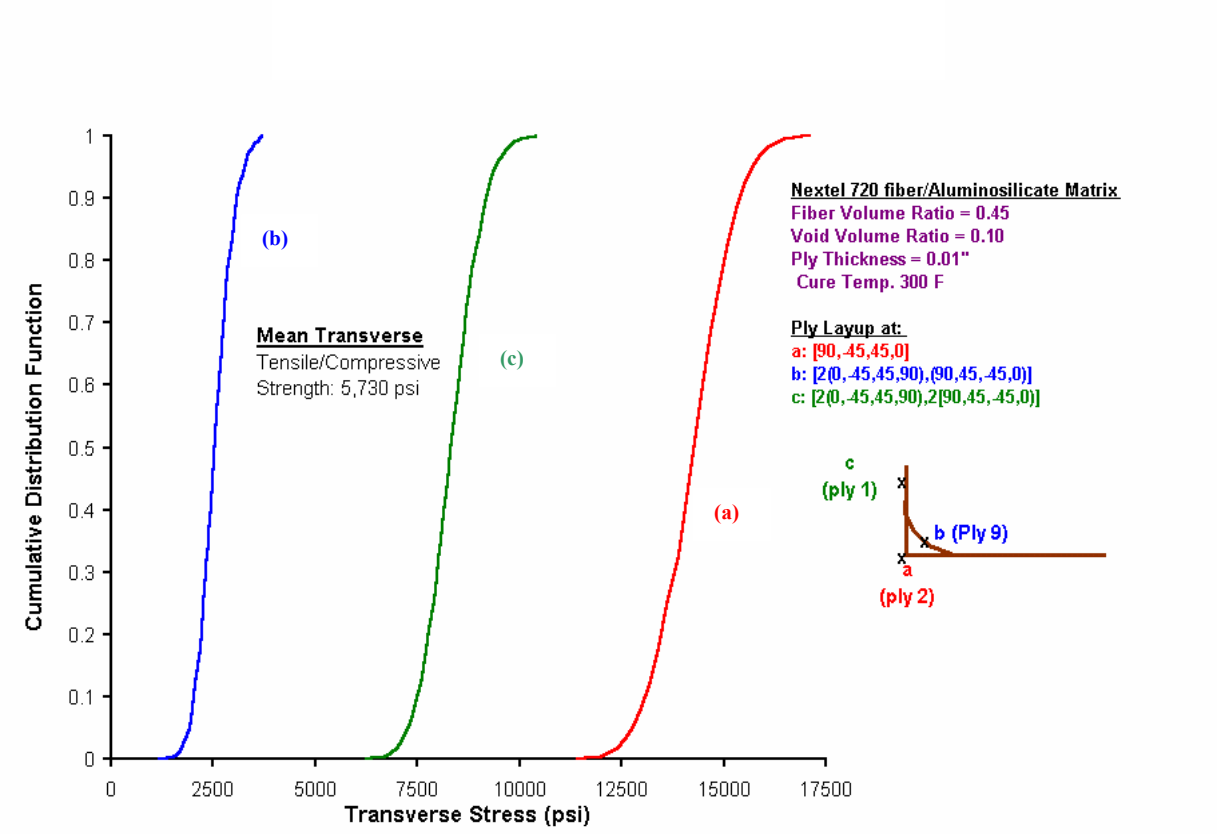

Figure 34. CMC flange – Probabilistic ply transverse stress (15 psi pressure)

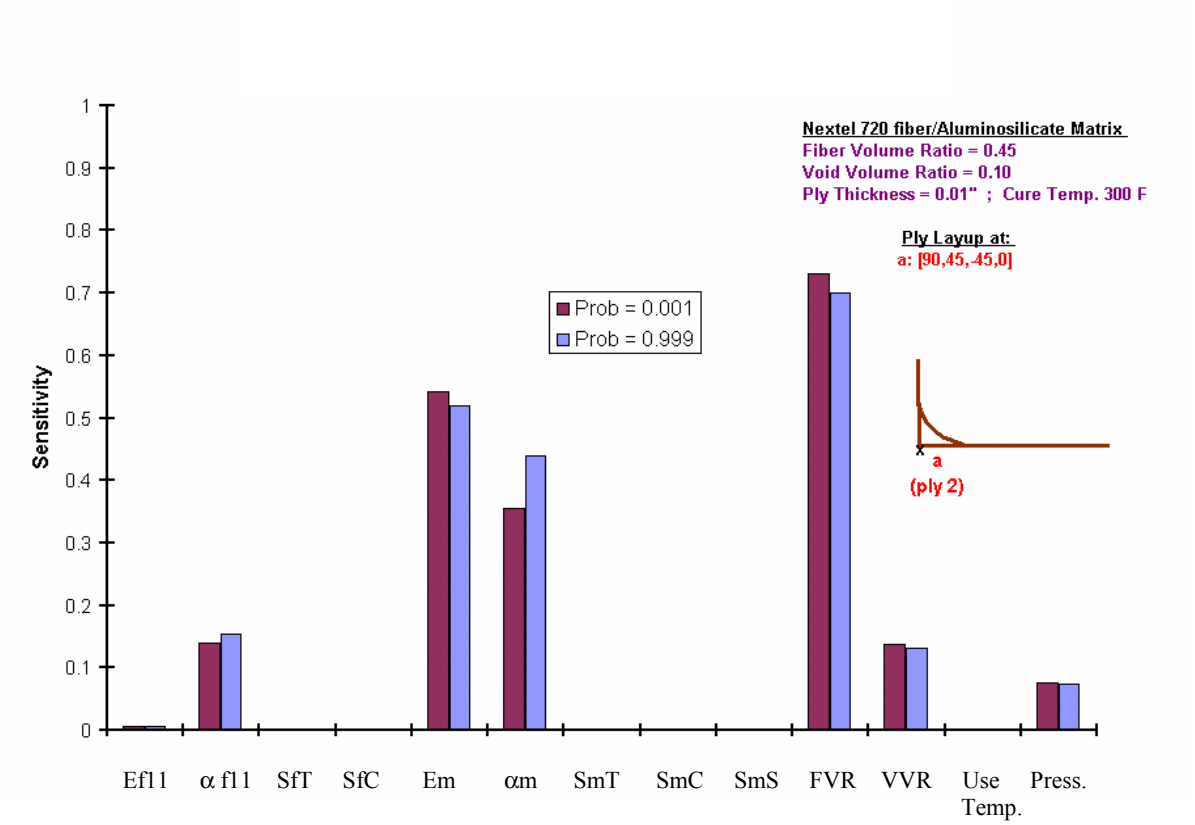

Figure 35. Probabilistic sensitivities for ply transverse stress criterion (15 psi pressure)

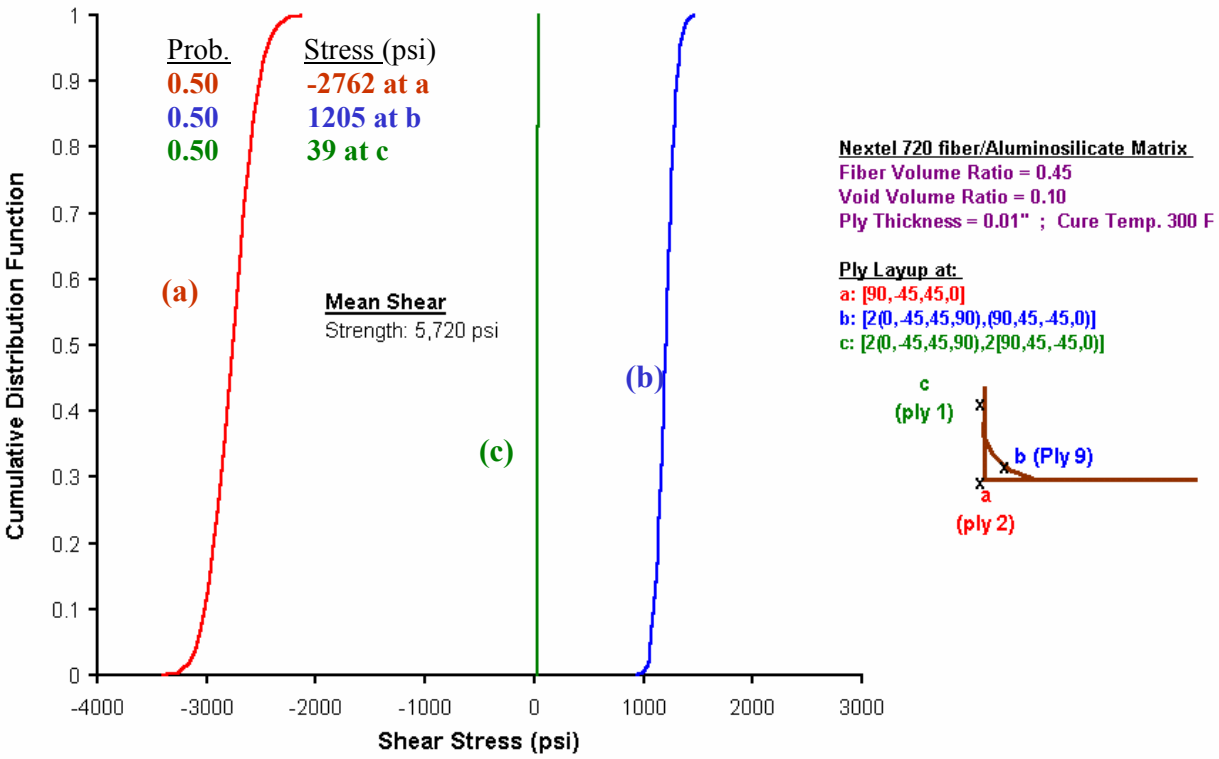

Figure 36. CMC flange – Probabilistic ply shear stress (15 psi pressure)

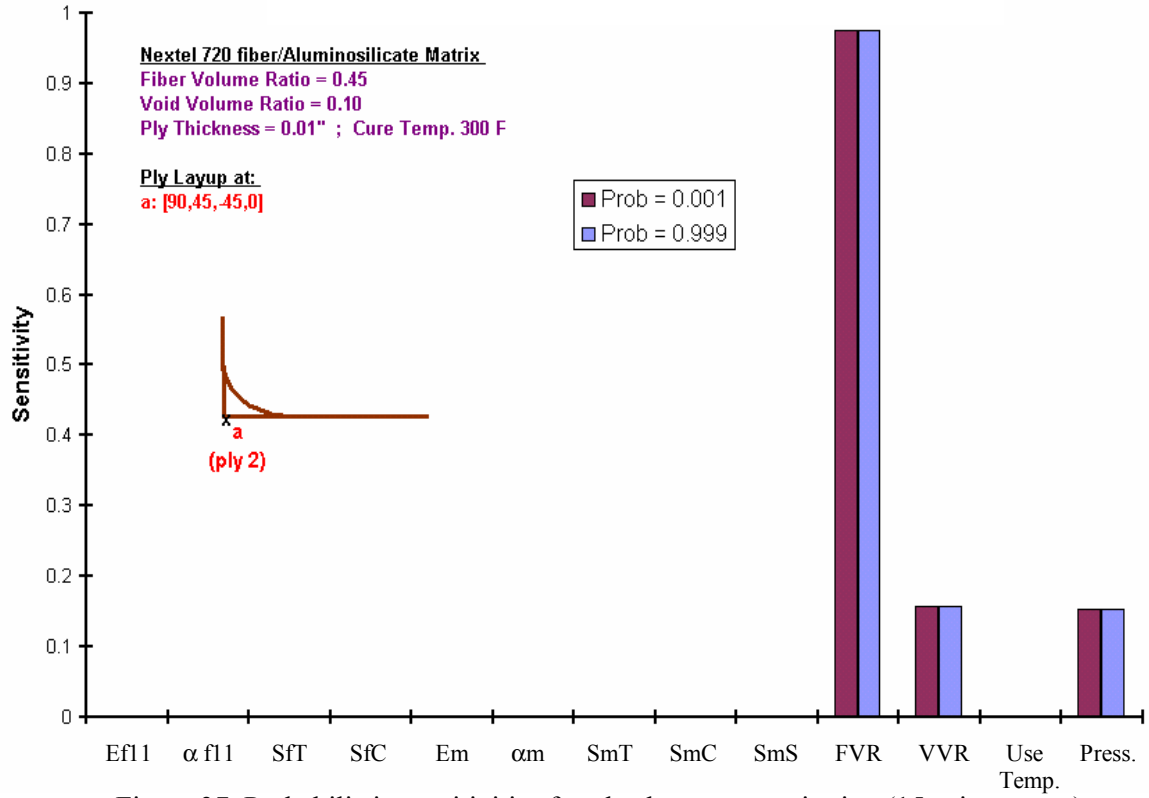

Figure 37. Probabilistic sensitivities for ply shear stress criterion (15 psi pressure)

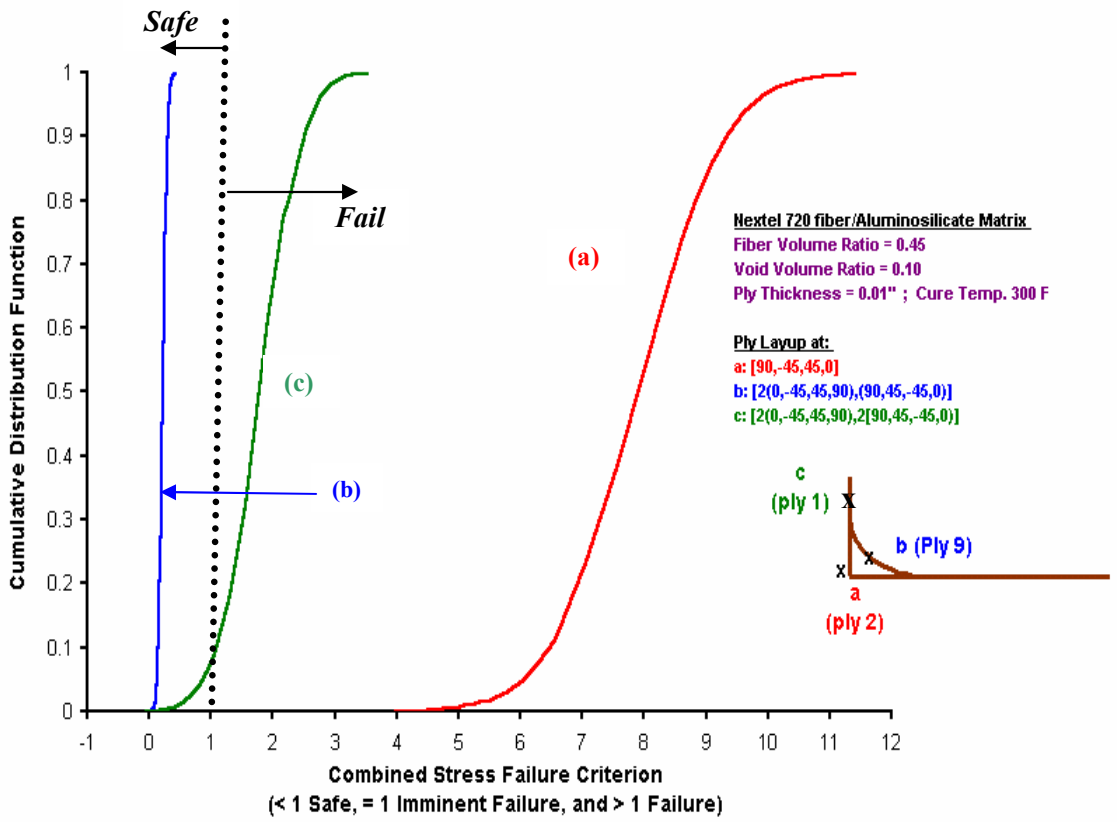

Figure 38. CMC flange - Probabilistic ply combined stress failure criterion (15 psi pressure)

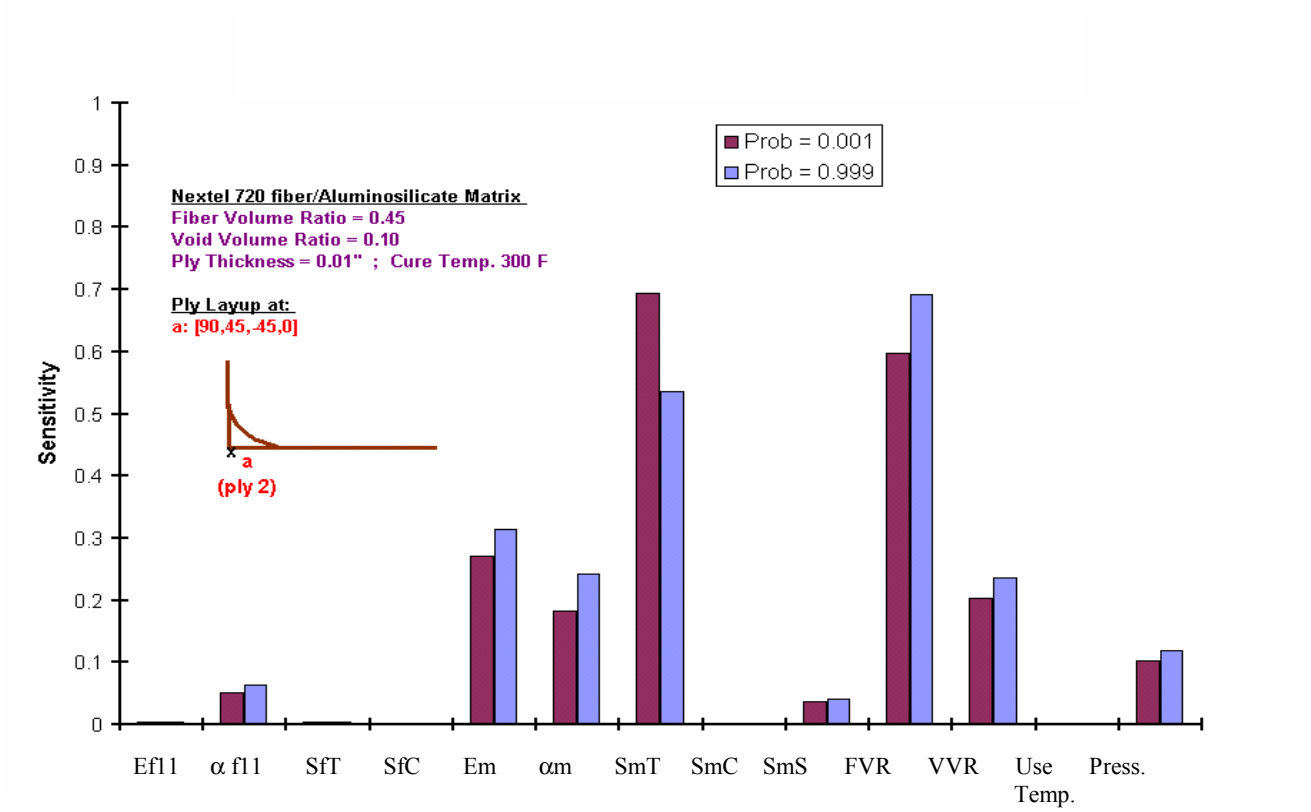

Figure 39. Probabilistic sensitivities for ply combined stress failure criterion (15 psi pressure)

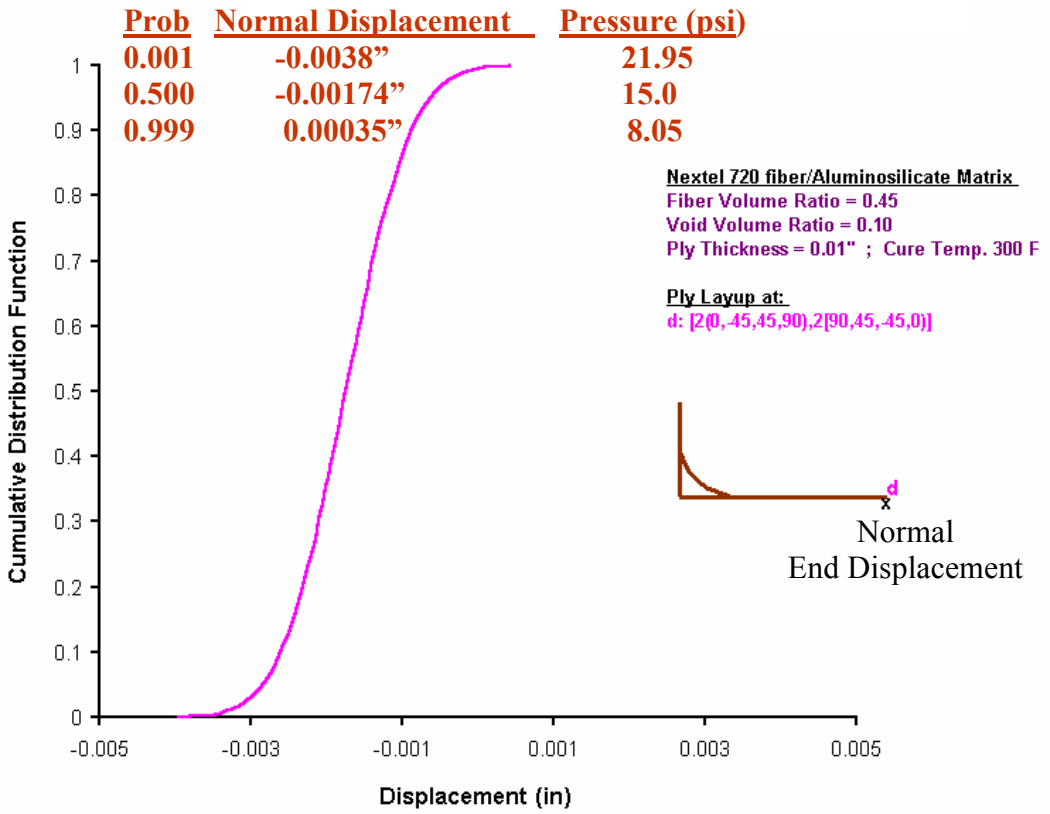

Figure 40. CMC flange – Probabilistic normal end displacement

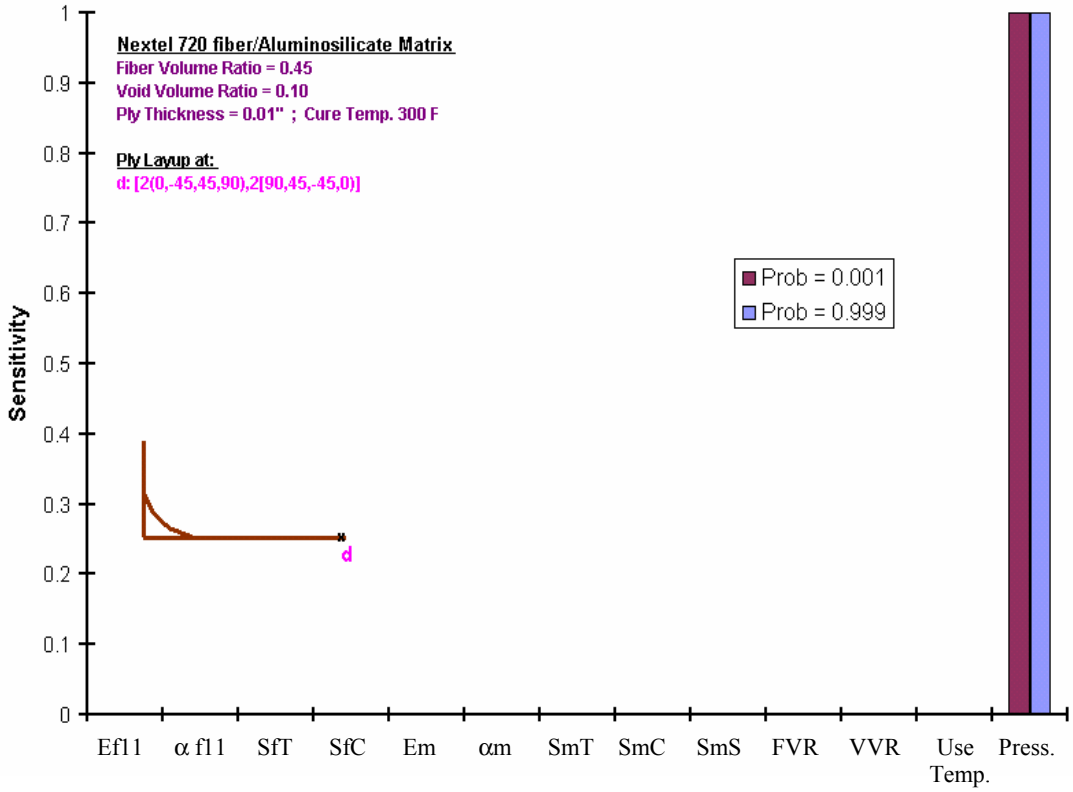

Figure 41. Probabilistic sensitivities of normal end displacement

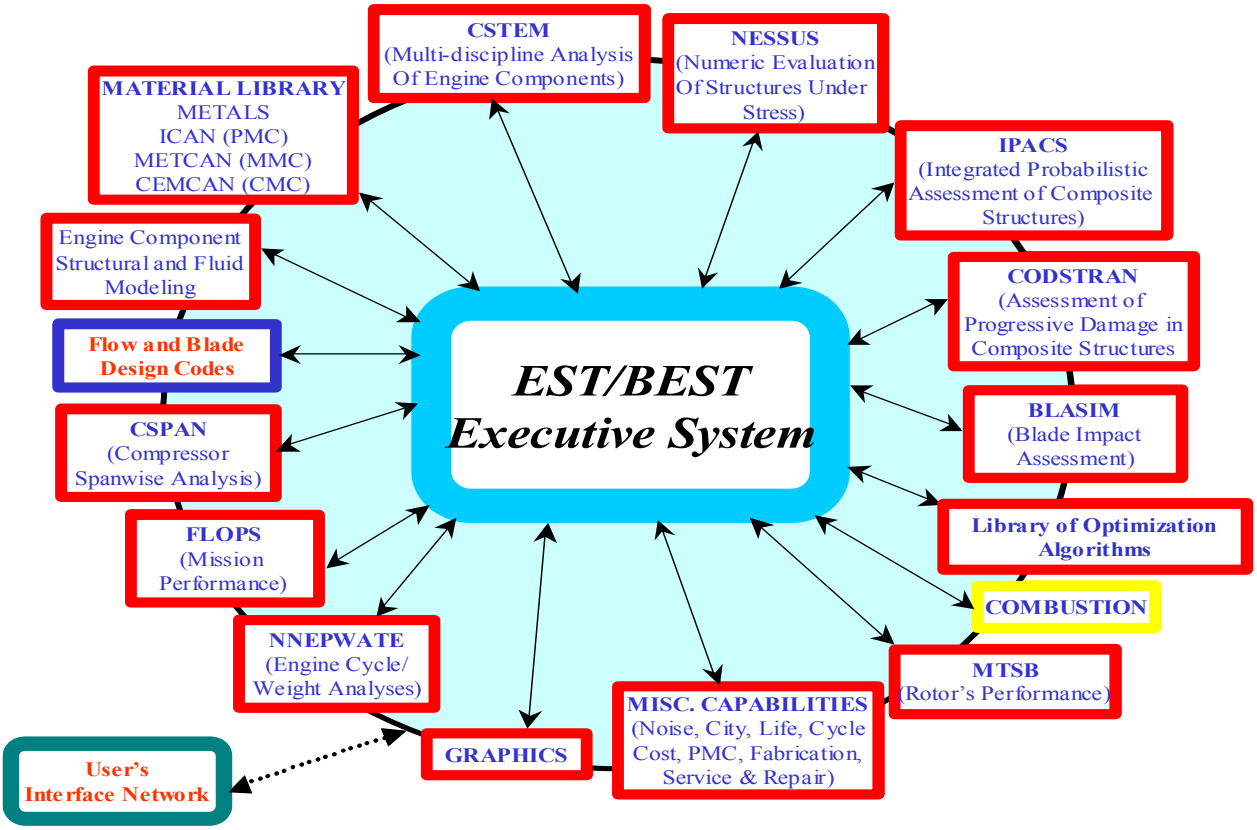

Figure 42. Modular chart of EST/BEST (Engine Structures Technology Benefit Estimator)

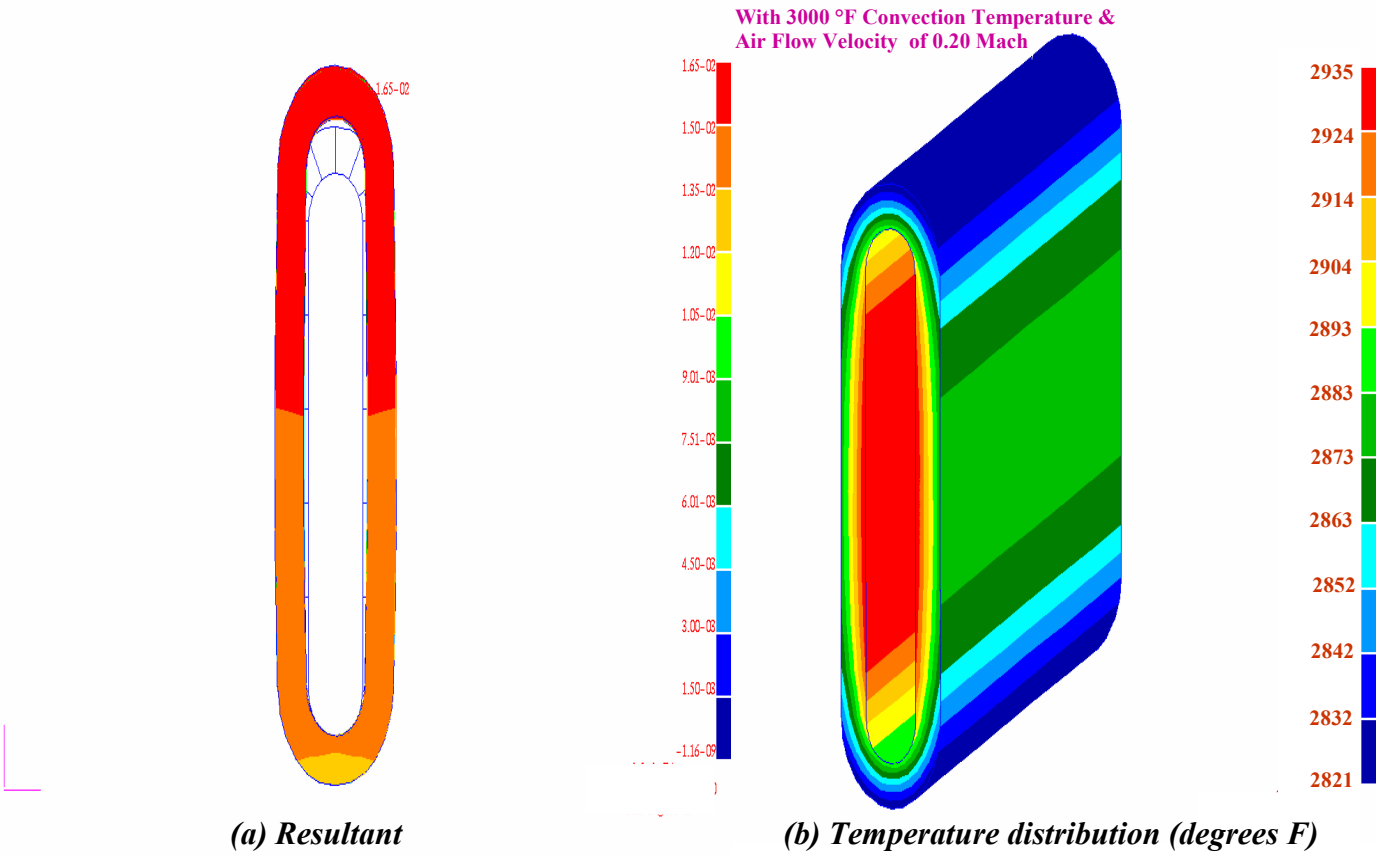

(a) Resultant *(b) Temperature distribution (degrees F)*

Figure 43. Deterministic coupled structural- thermal analysis of CMC tube

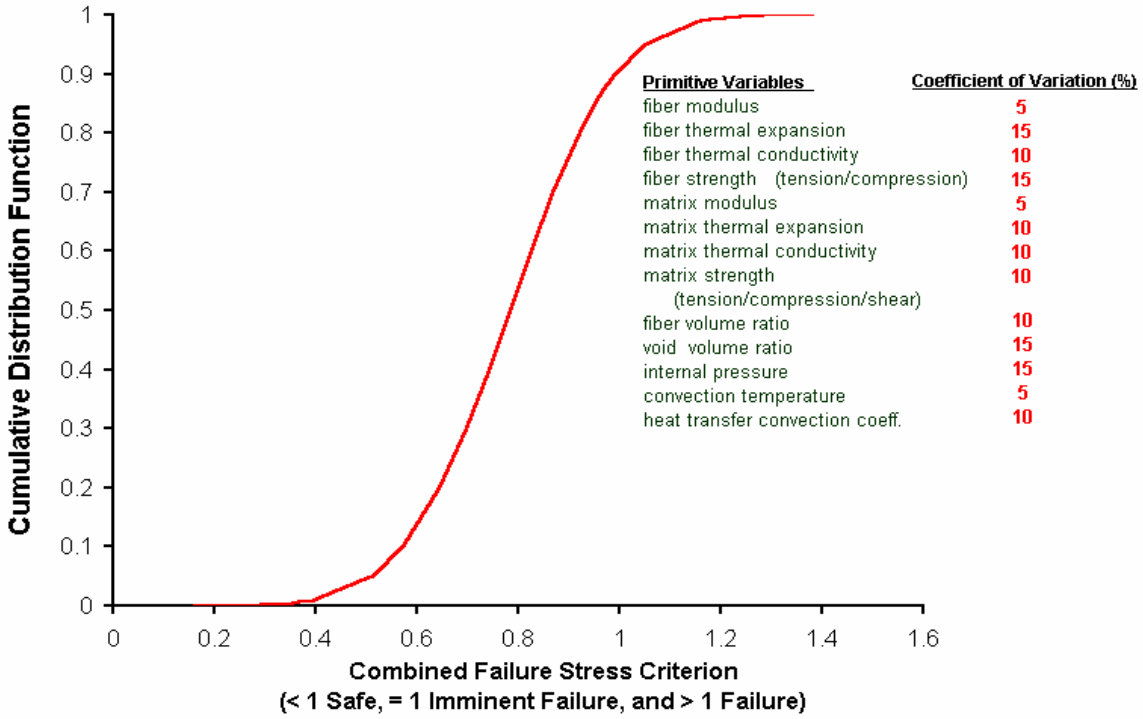

Figure 44. Probabilistic evaluation of combined stress failure criterion as a result of internal pressure and forced convection

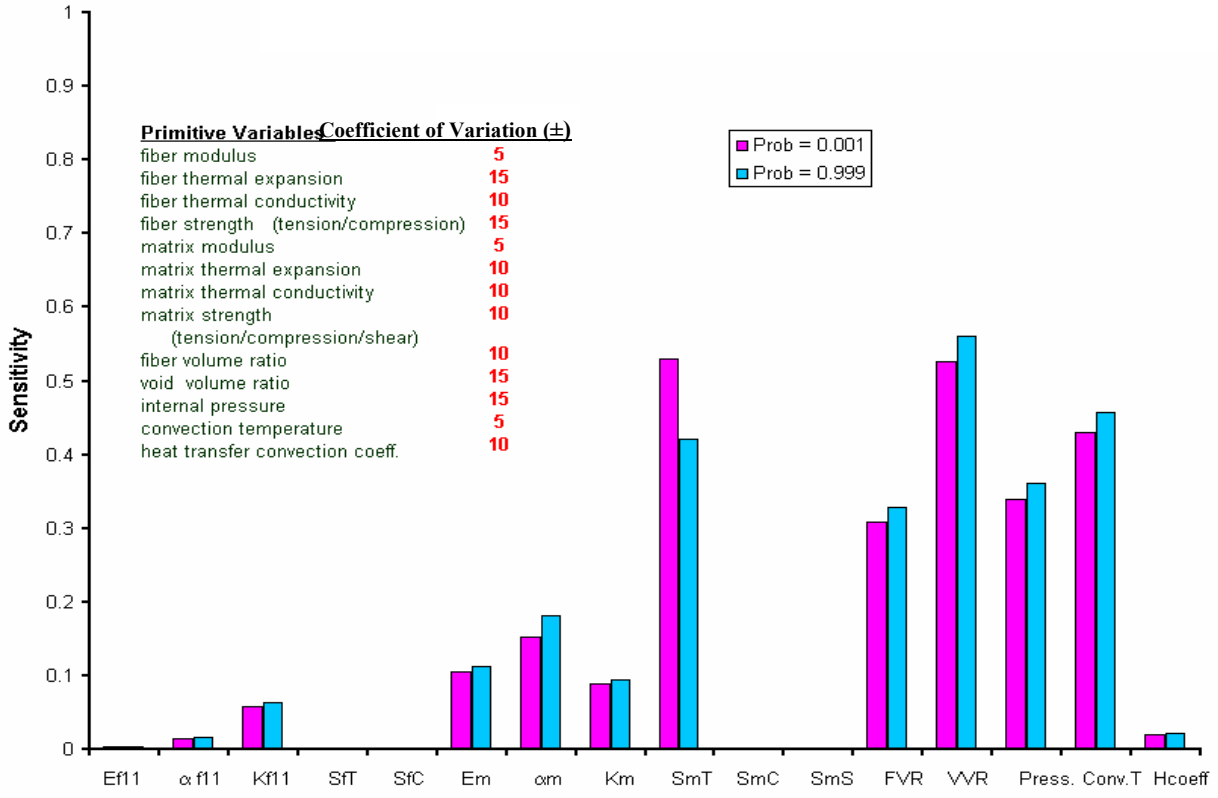

Figure 45. Probabilistic sensitivities of combined stress failure criterion as a result of internal pressure and forced convection

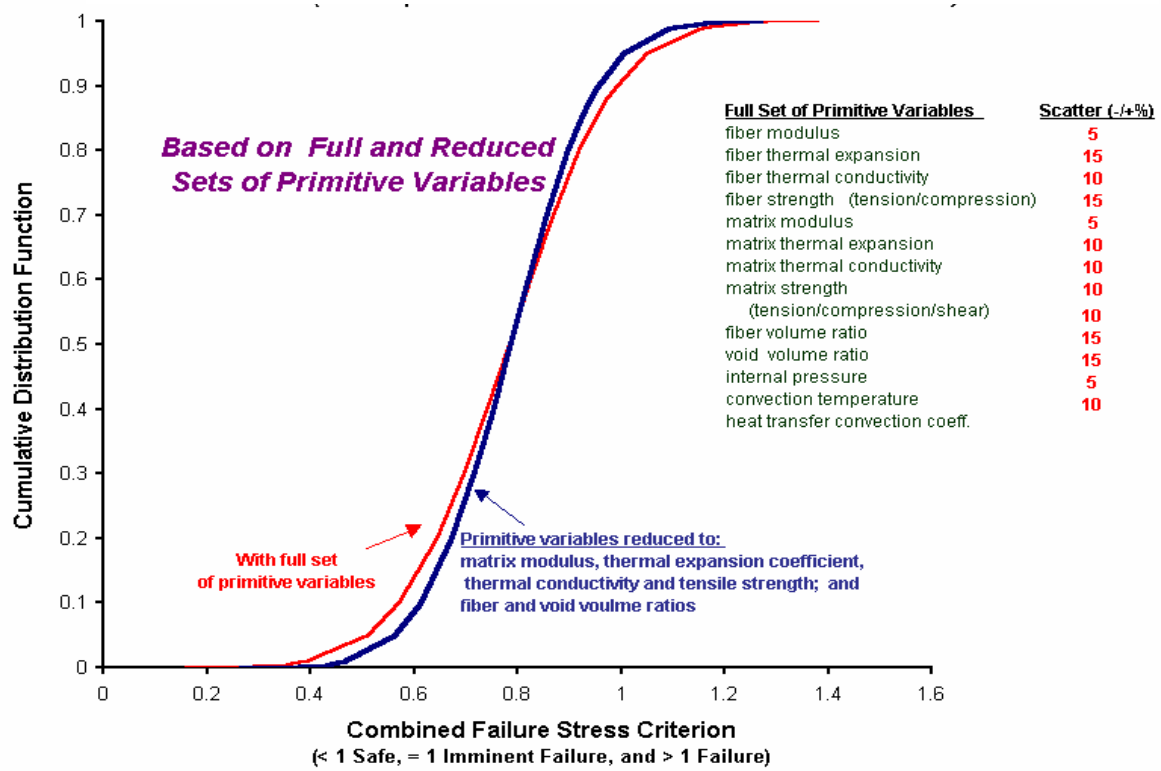

Figure 46. Probabilistic evaluation of combined stress failure criterion as a result of internal pressure and forced convection with reduced set of primitive variables

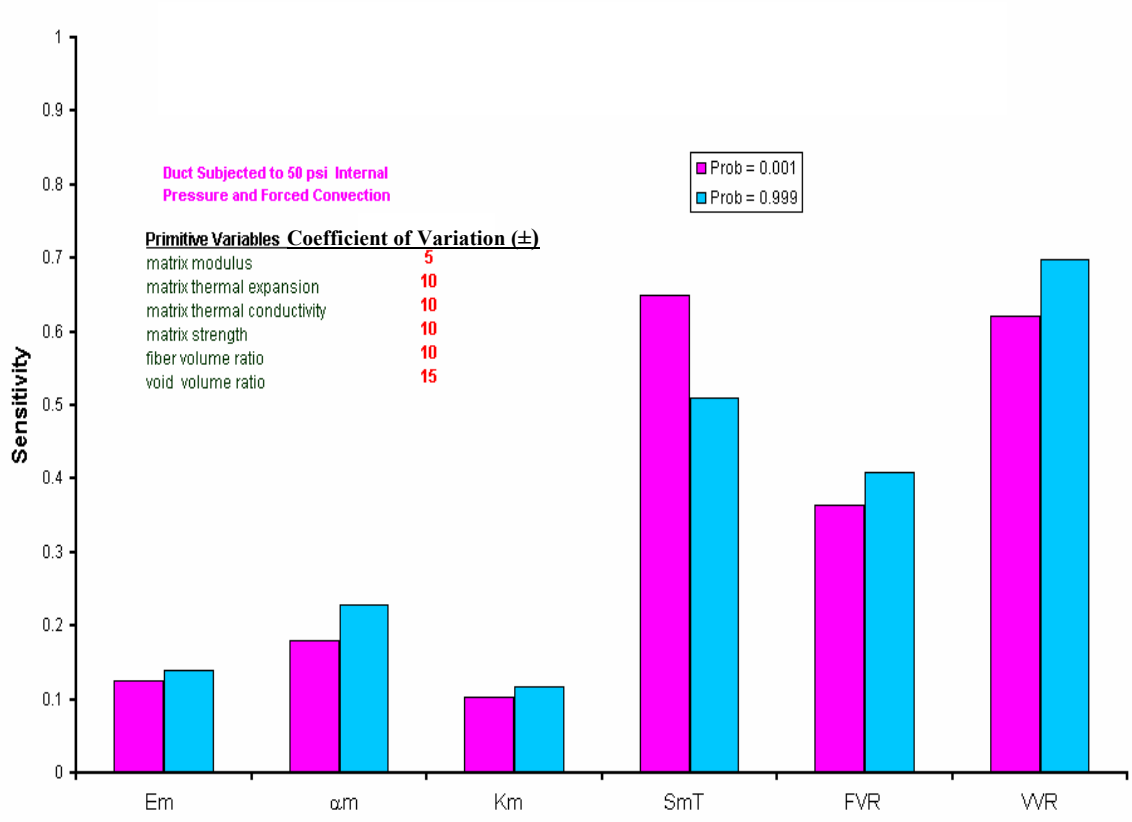

Figure 47. Probabilistic sensitivities of combined stress failure criterion as a result of internal pressure and forced convection with reduced set of primitive variables

REPORT DOCUMENTATION PAGE

Form Approved
OMB No. 0704-0188

1. AGENCY USE ONLY (*Leave blank*)	2. REPORT DATE	3. REPORT TYPE AND DATES COVERED
	July 2003	Technical Memorandum

4. TITLE AND SUBTITLE

Probabilistic Evaluation of Advanced Ceramic Matrix Composite Structures

5. FUNDING NUMBERS

WBS–22–708–48–11

6. AUTHOR(S)

Galib H. Abumeri and Christos C. Chamis

7. PERFORMING ORGANIZATION NAME(S) AND ADDRESS(ES)

National Aeronautics and Space Administration
John H. Glenn Research Center at Lewis Field
Cleveland, Ohio 44135–3191

8. PERFORMING ORGANIZATION REPORT NUMBER

E–14075

9. SPONSORING/MONITORING AGENCY NAME(S) AND ADDRESS(ES)

National Aeronautics and Space Administration
Washington, DC 20546–0001

10. SPONSORING/MONITORING AGENCY REPORT NUMBER

NASA TM—2003-212515

11. SUPPLEMENTARY NOTES

Galib H. Abumeri, QSS Group, Inc., Cleveland, Ohio 44135; and Christos C. Chamis, NASA Glenn Research Center. Responsible person, Christos C. Chamis, organization code 5000, 216–433–3252.

12a. DISTRIBUTION/AVAILABILITY STATEMENT

Unclassified - Unlimited
Subject Category: 39 Distribution: Nonstandard

Available electronically at http://gltrs.grc.nasa.gov

This publication is available from the NASA Center for AeroSpace Information, 301–621–0390.

12b. DISTRIBUTION CODE

13. ABSTRACT ***(Maximum 200 words)***

The objective of this report is to summarize the deterministic and probabilistic structural evaluation results of two structures made with advanced ceramic composites (CMC): internally pressurized tube and uniformly loaded flange. The deterministic structural evaluation includes stress, displacement, and buckling analyses. It is carried out using the finite element code MHOST, developed for the 3-D inelastic analysis of structures that are made with advanced materials. The probabilistic evaluation is performed using the integrated probabilistic assessment of composite structures computer code IPACS. The affects of uncertainties in primitive variables related to the material, fabrication process, and loadings on the material property and structural response behavior are quantified. The primitive variables considered are: thermo-mechanical properties of fiber and matrix, fiber and void volume ratios, use temperature, and pressure. The probabilistic structural analysis and probabilistic strength results are used by IPACS to perform reliability and risk evaluation of the two structures. The results will show that the sensitivity information obtained for the two composite structures from the computational simulation can be used to alter the design process to meet desired service requirements. In addition to detailed probabilistic analysis of the two structures, the following were performed specifically on the CMC tube: (1) predicted the failure load and the buckling load, (2) performed coupled non-deterministic multi-disciplinary structural analysis, and (3) demonstrated that probabilistic sensitivities can be used to select a reduced set of design variables for optimization.

14. SUBJECT TERMS

Uncertainties; Sensitivities; Stress; Strength; Optimization; Multi-discipline

15. NUMBER OF PAGES

53

16. PRICE CODE

17. SECURITY CLASSIFICATION OF REPORT	18. SECURITY CLASSIFICATION OF THIS PAGE	19. SECURITY CLASSIFICATION OF ABSTRACT	20. LIMITATION OF ABSTRACT
Unclassified	Unclassified	Unclassified	